

Constraining cosmological models with surveys of galaxy clusters

Barbara Sartoris

In collaboration with J. Weller (LMU), S. Borgani (University of Trieste), P. Rosati (ESO)

Ludwig-Maximilians University Munich

Excellence Cluster Universe of Munich

Heidelberg, 22 VI 2012

Cosmology with clusters of galaxies

Galaxy clusters as cosmological probes

Growth tests

Geometrical tests

Forecasts from future surveys

The importance of the observable mass calibration

Combination of power

spectrum and number density

Dark Energy constraints

Non Gaussian constraints

Cosmological constraints from current cluster surveys

Massive high-redshift clusters

High-redshift ($z > 0.8$) mass function

Cosmology with clusters of galaxies

Galaxy clusters as cosmological probes

Growth tests

Geometrical tests

Forecasts from future surveys

The importance of the observable mass calibration

Combination of power

spectrum and number density

Dark Energy constraints

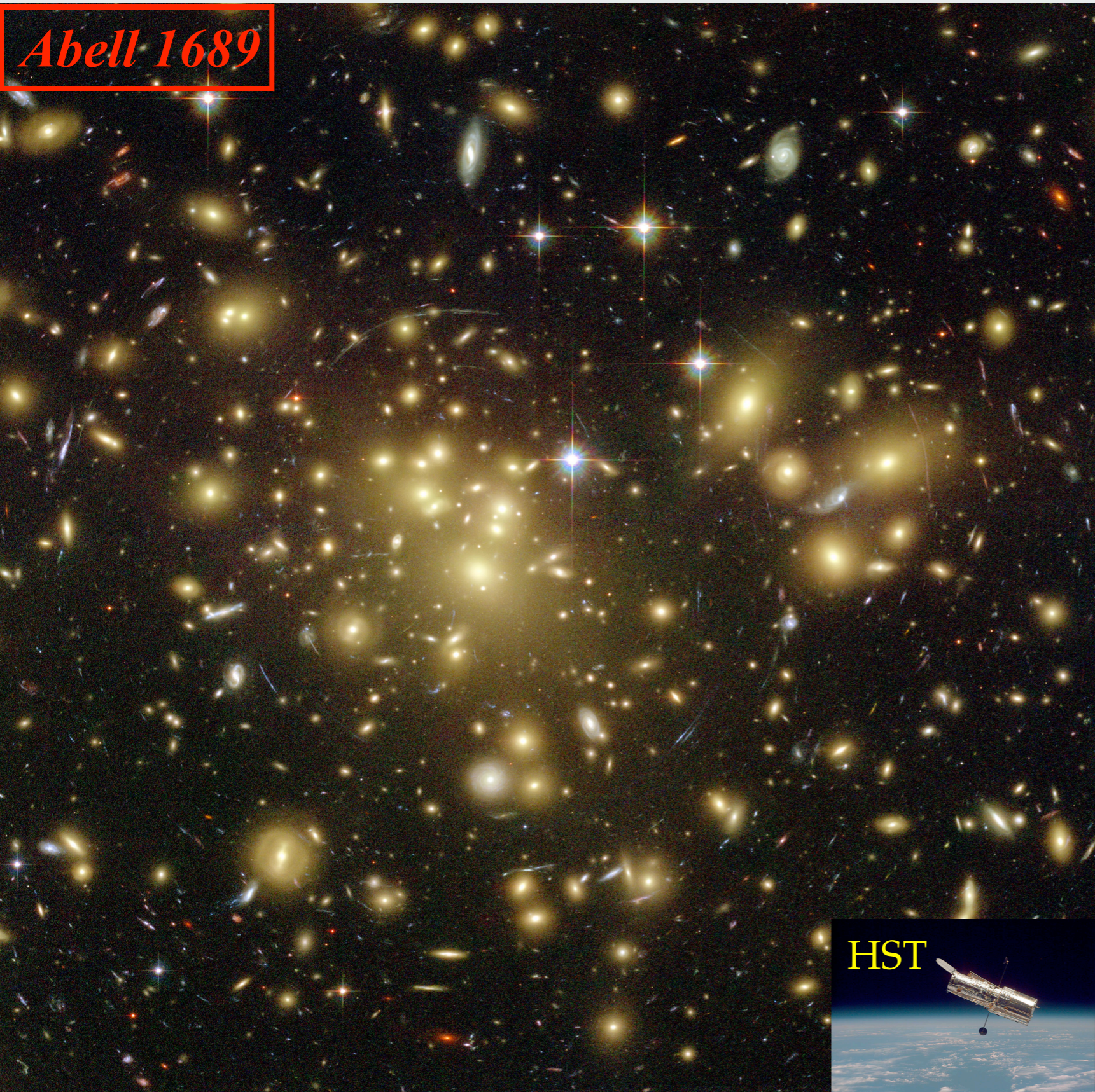
Non Gaussian constraints

Cosmological constraints from current cluster surveys

Massive high-redshift clusters

High-redshift ($z > 0.8$) mass function

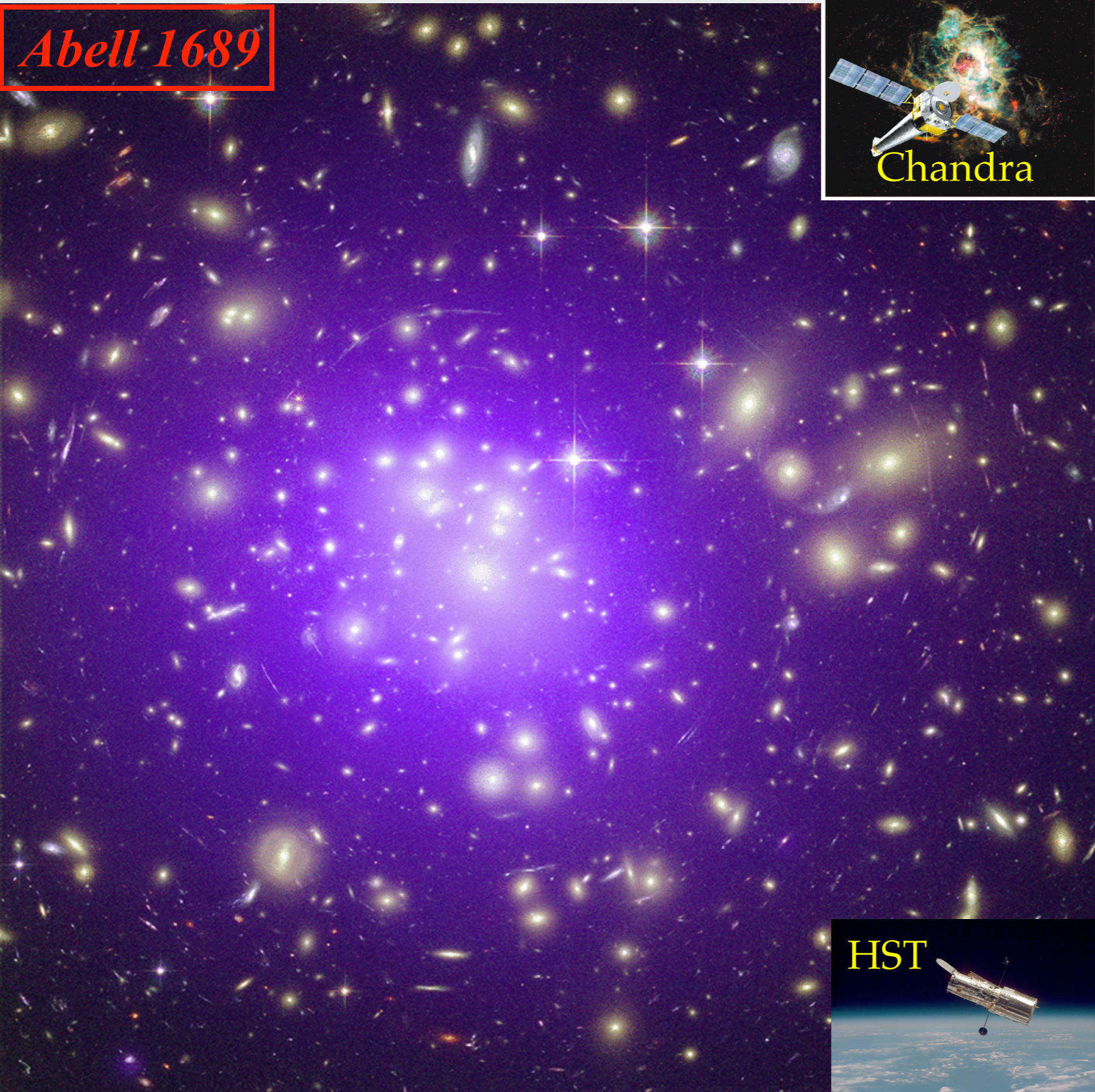
Abell 1689



Observing a galaxy cluster

- Concentration of
~103 galaxies
- $\sigma_v \sim 500-1000 \text{ km s}^{-1}$
- Size: ~1-2 Mpc
- Mass: $\sim 10^{14} M_{\odot}$

Abell 1689

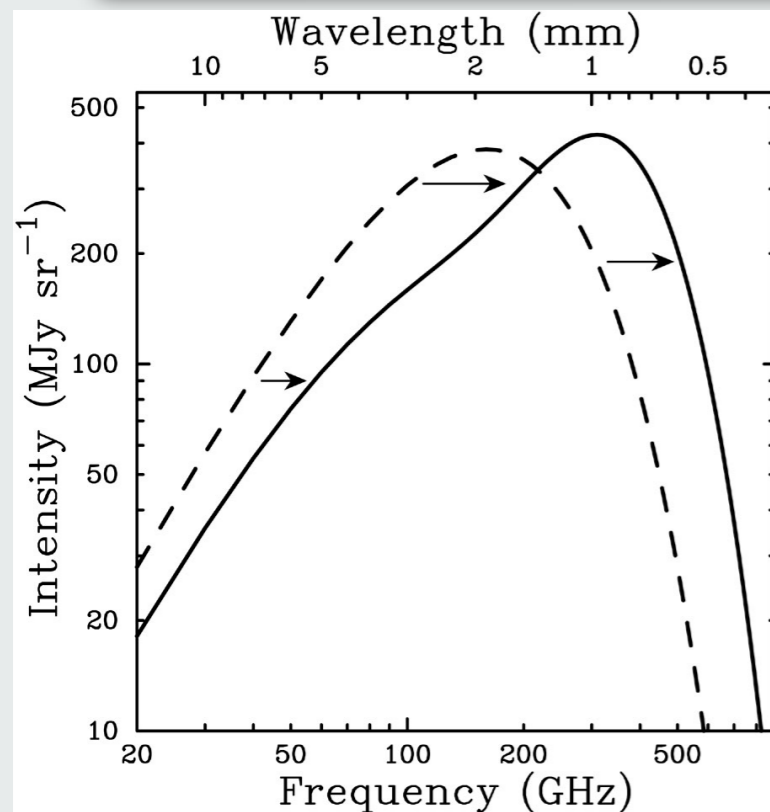


Observing a galaxy cluster

- Concentration of
~103 galaxies
- $\sigma_v \sim 500-1000 \text{ km s}^{-1}$
- Size: ~1-2 Mpc
- Mass: $\sim 10^{14} M_\odot$

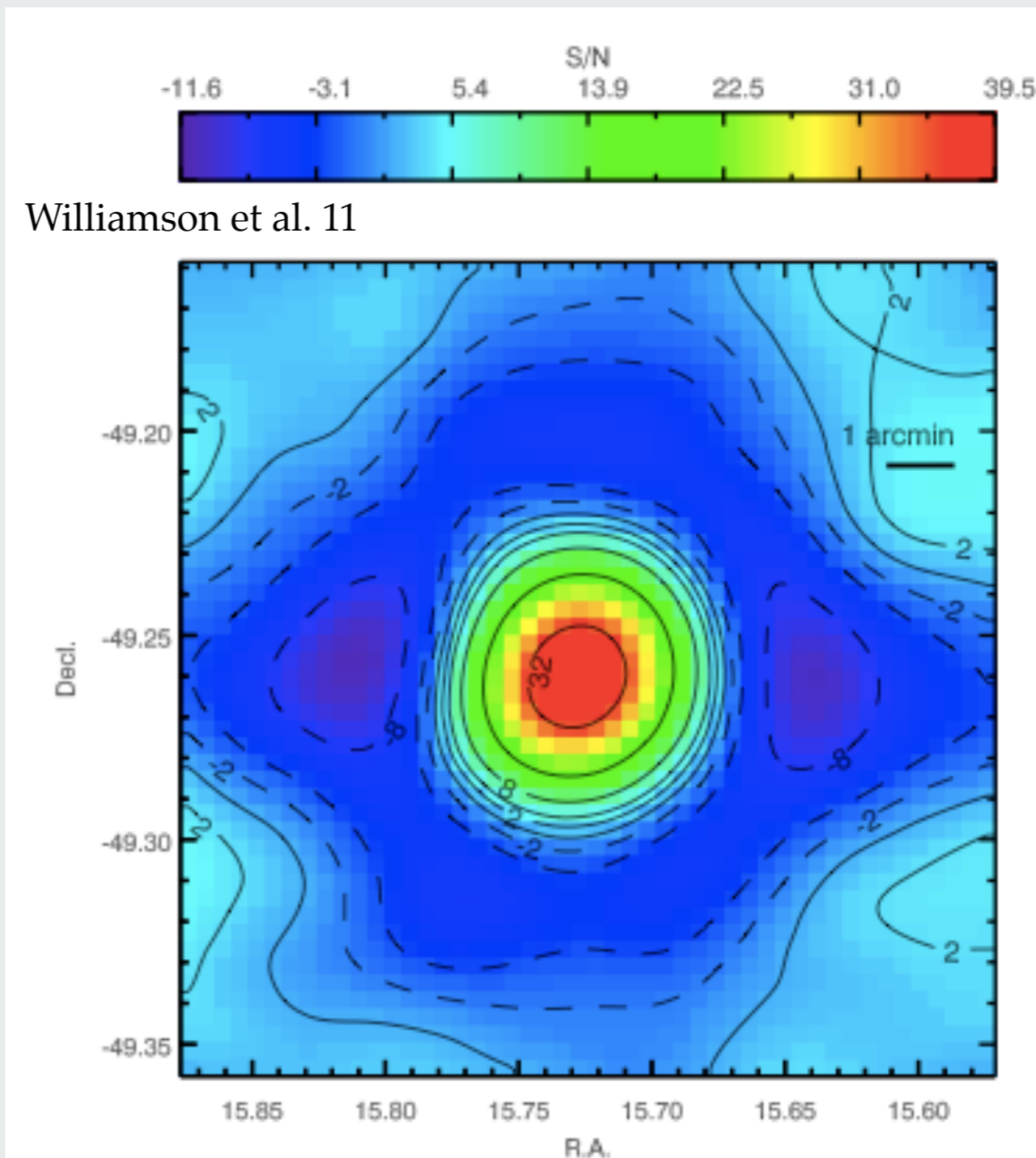
- ICM temperature:
 $T_x \sim 2-10 \text{ keV}$
fully ionized plasma;
- Therm bremsstrahlung:
 $n_e \sim 10^{-2}-10^{-4} \text{ cm}^{-3}$
 $L_x \sim 10^{45} \text{ erg s}^{-1}$

Observations of the Sunyaev-Zeldovich Effect



Inverse Compton scattering of CMB photons off the ICM electrons

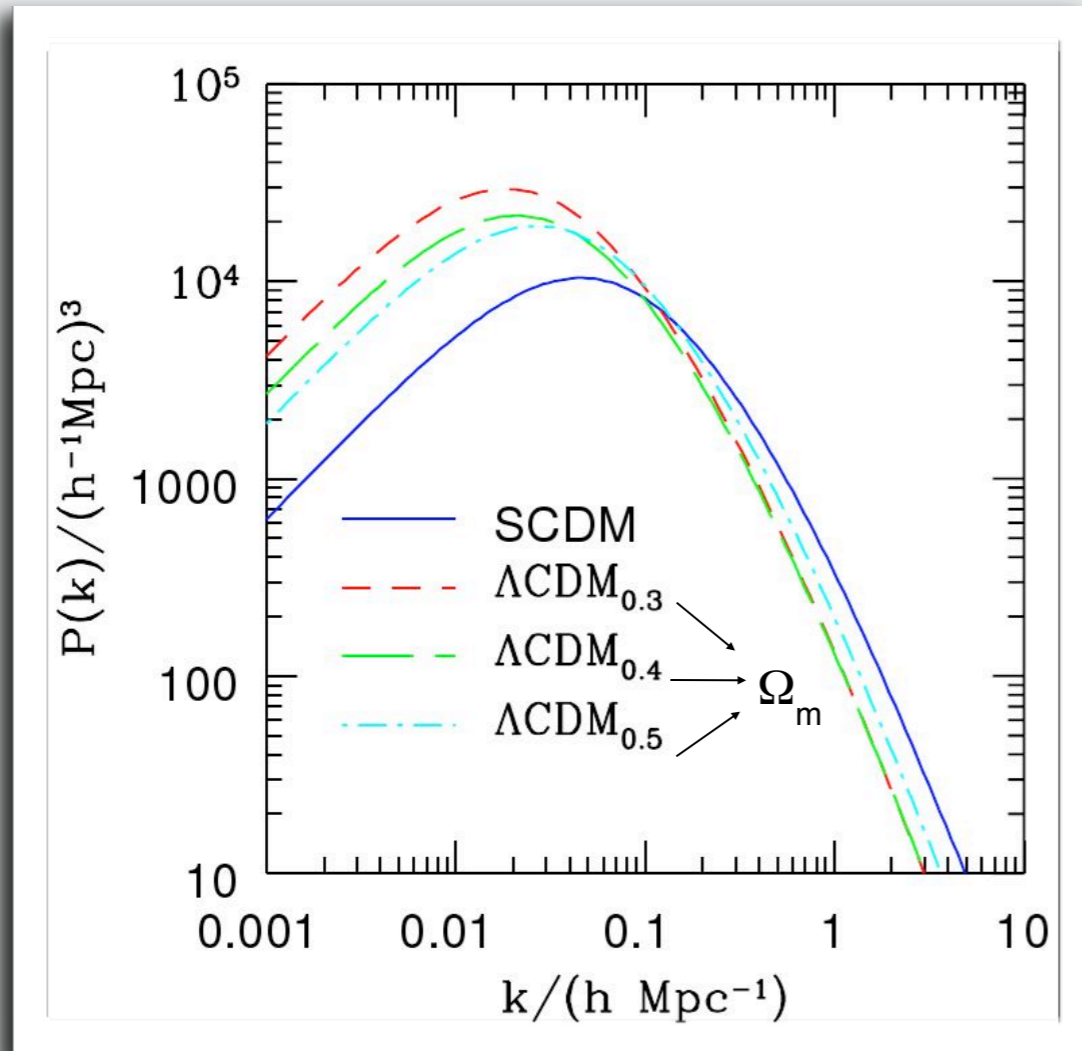
SPT cluster $z=0.78$



- Signal virtually independent of redshift.
- Proportional to the l.o.s. integration of $n_e T_e \sim$ pressure
- Survey for cluster detection are now producing results (e.g. ACT, SPT, Planck).

Constrain cosmological parameters with power spectrum

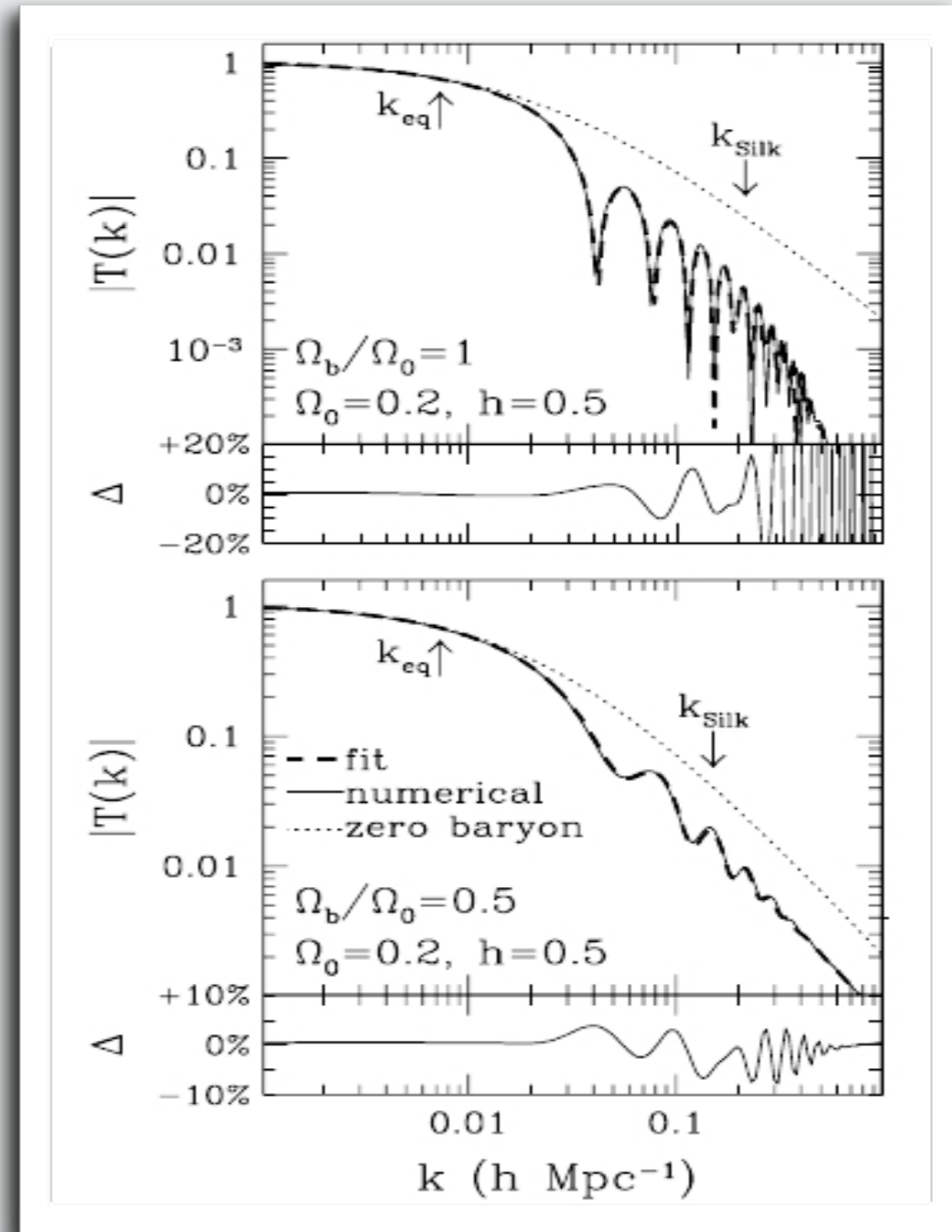
Power spectrum shape



$$P(k, z) = T^2(k) D^2(z) P_{in}(k)$$

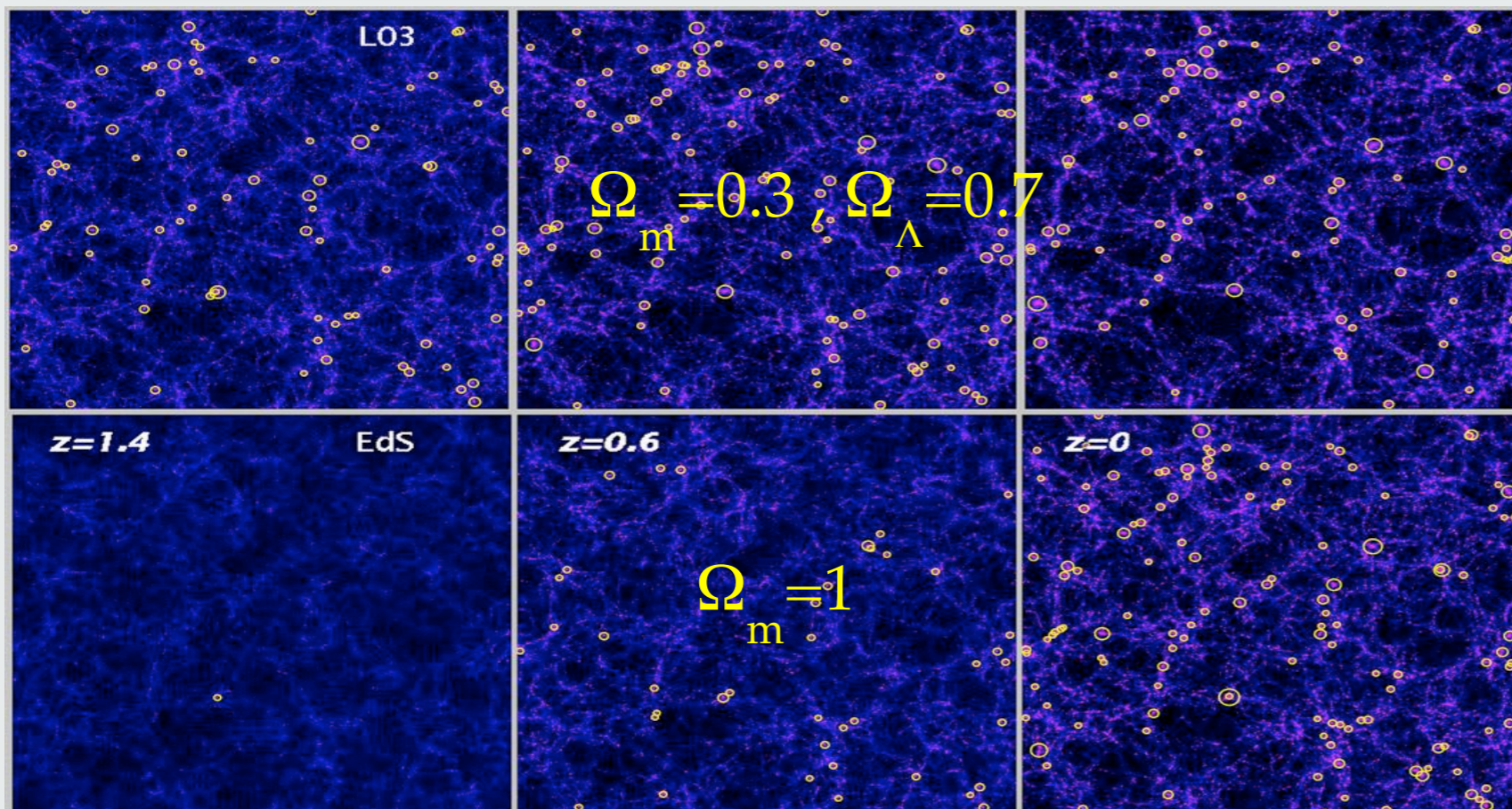
Borgani et al 1997

Barionic Acoustic Oscillations



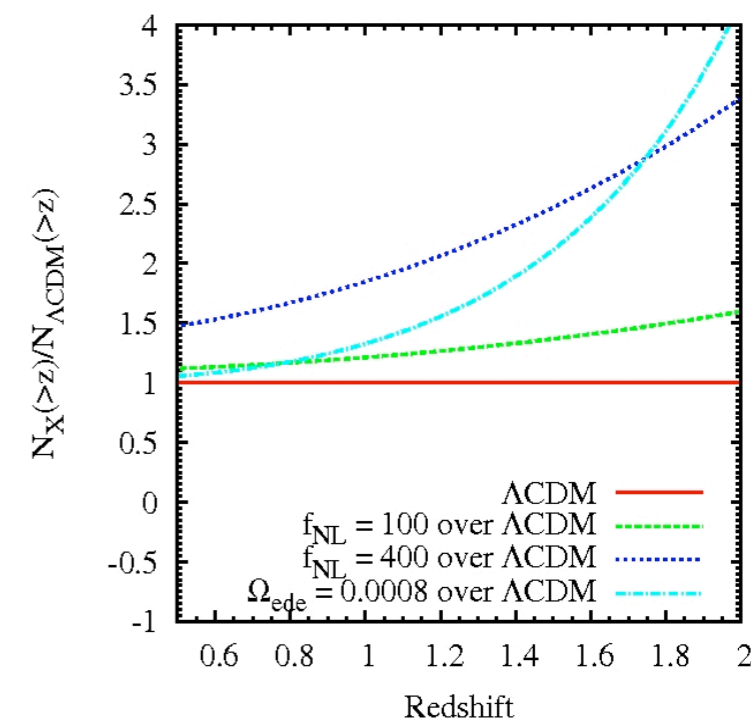
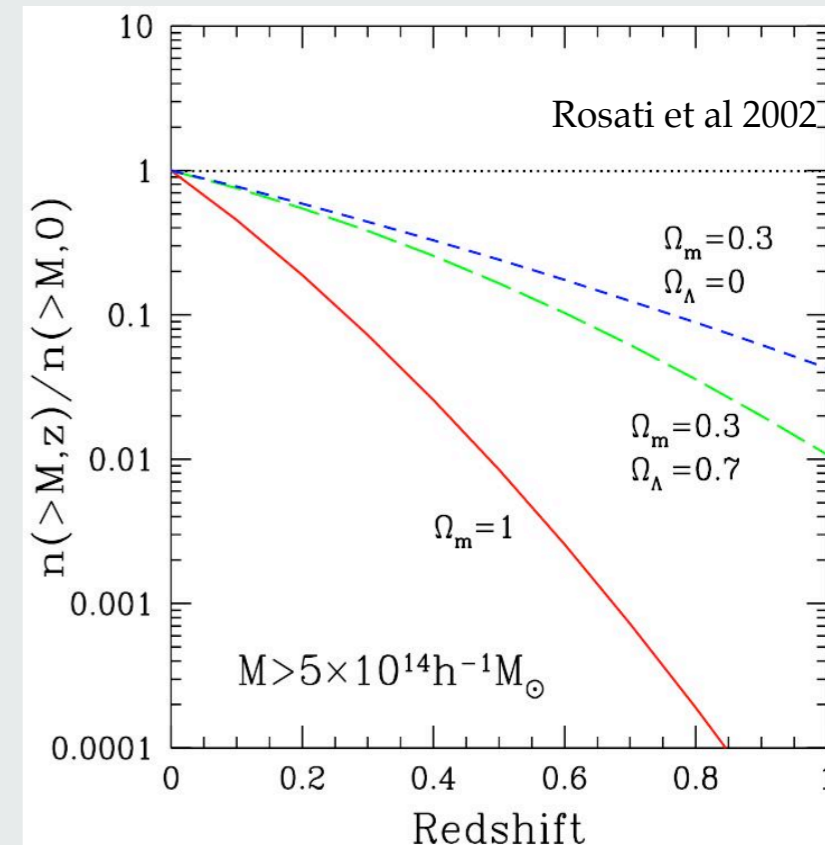
Eisenstein & Hu 1998

Constrain cosmological parameters with clusters number density



Borgani&Guzzo 2001

$$N_{l,m} = \Delta\Omega \int_{z_l}^{z_{l+1}} dz \frac{dV}{dzd\Omega} \int_{M_{l,m}^{ob}}^{M_{l,m+1}^{ob}} dM^{ob} \int_0^\infty dM n(M, z) p(M^{ob} || M) .$$



Cosmological information from cluster number density

$$\frac{dN(X; z)}{dXdz}$$

Number of clusters of given observable X and redshift z within the survey area

- Friedmann background:

$$\frac{dV}{dz}$$

Priors on cosmological parameters Ω_i from CMB, SNIa,

- Growth history:

$$\frac{dn(M, z, \Omega_i)}{dM}$$

Calibrated with N-body simulations

- Astrophysics:

$$\frac{dM}{dX}$$

Priors on “mass parameters” p_j from follow-up observations and / or cosmological simulations

Cosmology with clusters of galaxies

Galaxy clusters as cosmological probes

Growth tests

Geometrical tests

Forecasts from future surveys

The importance of the observable mass calibration

Combination of power

spectrum and number density

Dark Energy constraints

Non Gaussian constraints

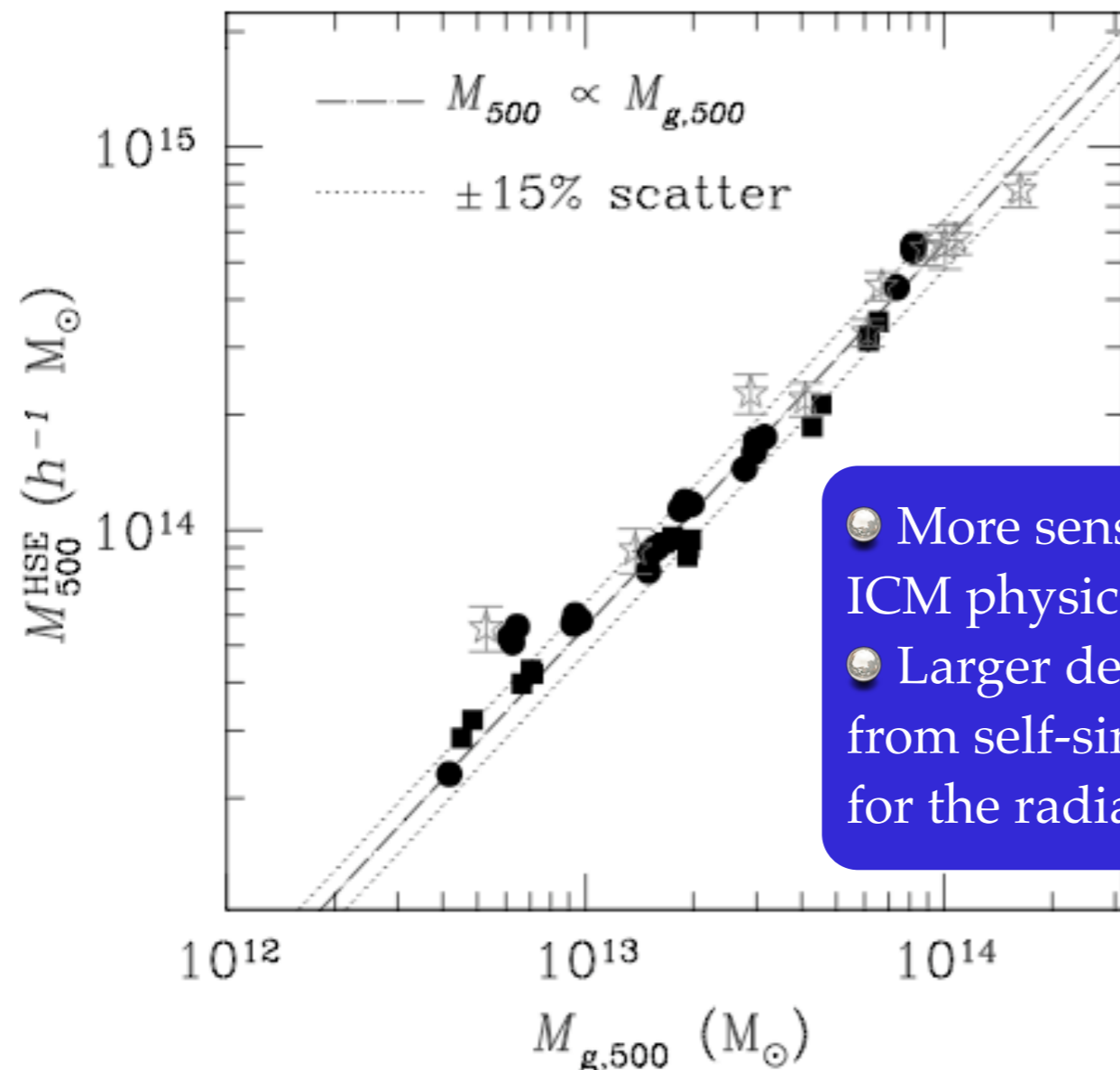
Cosmological constraints from current cluster surveys

Massive high-redshift clusters

High-redshift ($z > 0.8$) mass function

Observable - mass relations

Self-similar Gas-Cluster Mass relation from simulations



- More sensitive to ICM physics
- Larger deviations from self-similar slope for the radiative runs

Assumptions:

- ICM evolves in gravitational potential of DM:

$$f_{\text{gas}} = \frac{M_{\text{gas}}}{M_{200}}$$

- ICM is hydrostatic equilibrium \rightarrow Virial Theorem

$$M_{200} \propto h^{-1}(z) T^{3/2}$$

- bremsstrahlung emission

$$L_X \propto h(z) T^2$$

Nagai, Kravtsov & Vikhlinin 2007

Observable - mass relations

Self-similar Gas-Cluster Mass relation from simulations

Assumptions:

- ICM evolves in gravitational potential of DM:

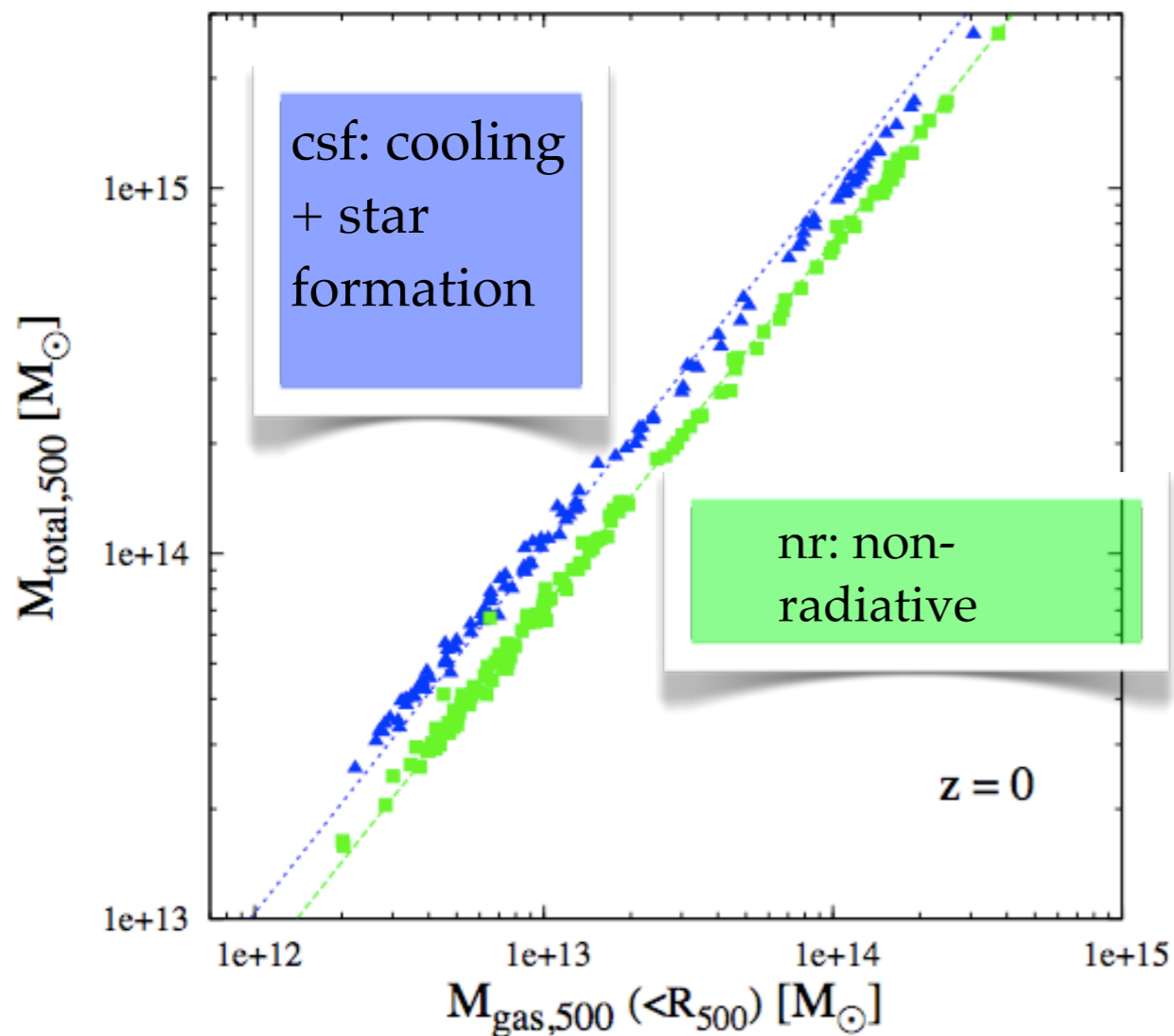
$$f_{\text{gas}} = \frac{M_{\text{gas}}}{M_{200}}$$

- ICM is hydrostatic equilibrium → Virial Theorem

$$M_{200} \propto h^{-1}(z) T^{3/2}$$

- bremsstrahlung emission

$$L_X \propto h(z) T^2$$



ve to
tions
ar slope
e runs

Observable - mass relations

Self-similar Mass-Temperature relation from simulations

Assumptions:

- ICM evolves in gravitational potential of DM:

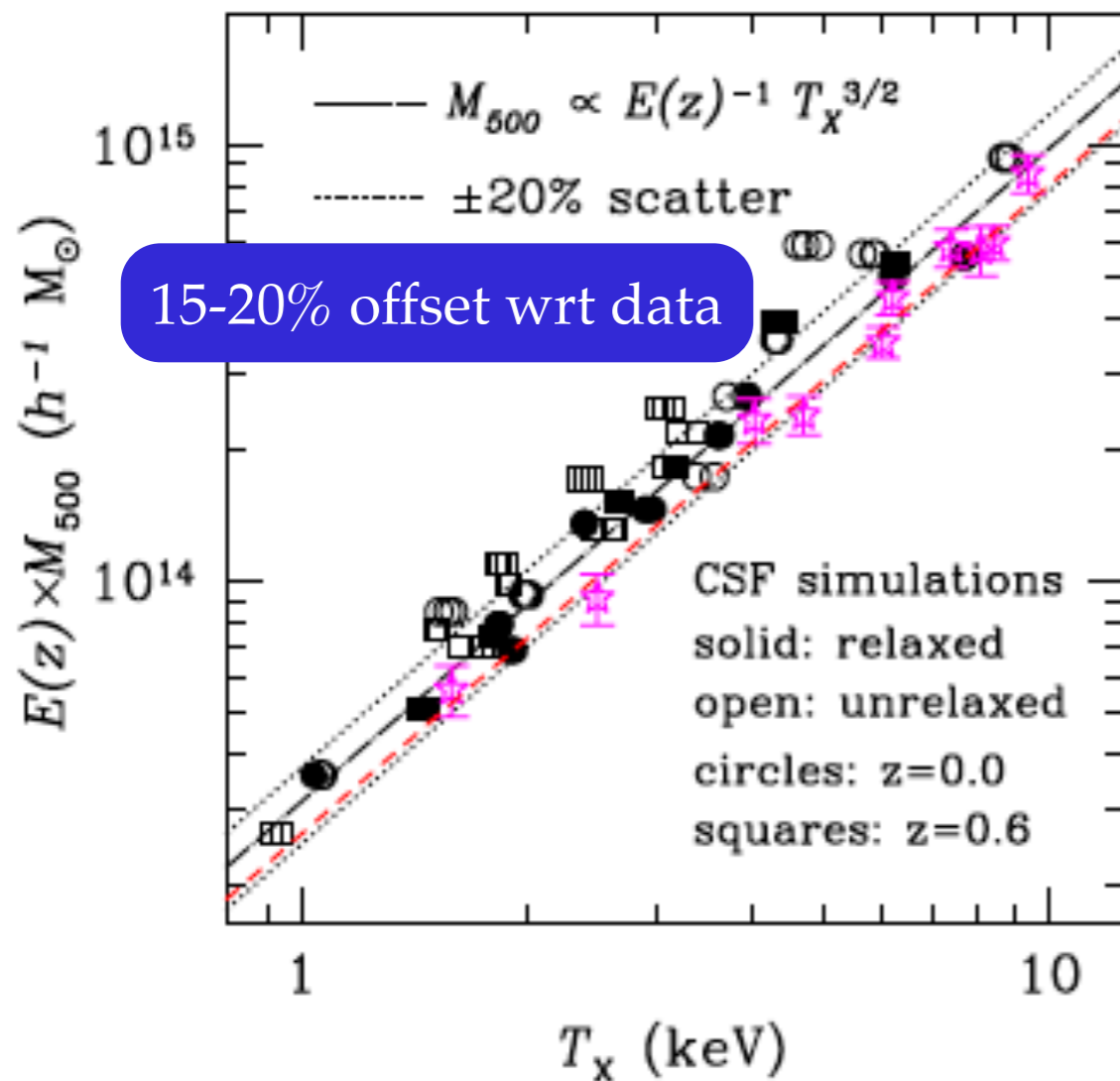
$$f_{\text{gas}} = \frac{M_{\text{gas}}}{M_{200}}$$

- ICM is hydrostatic equilibrium → Virial Theorem

$$M_{200} \propto h^{-1}(z) T^{3/2}$$

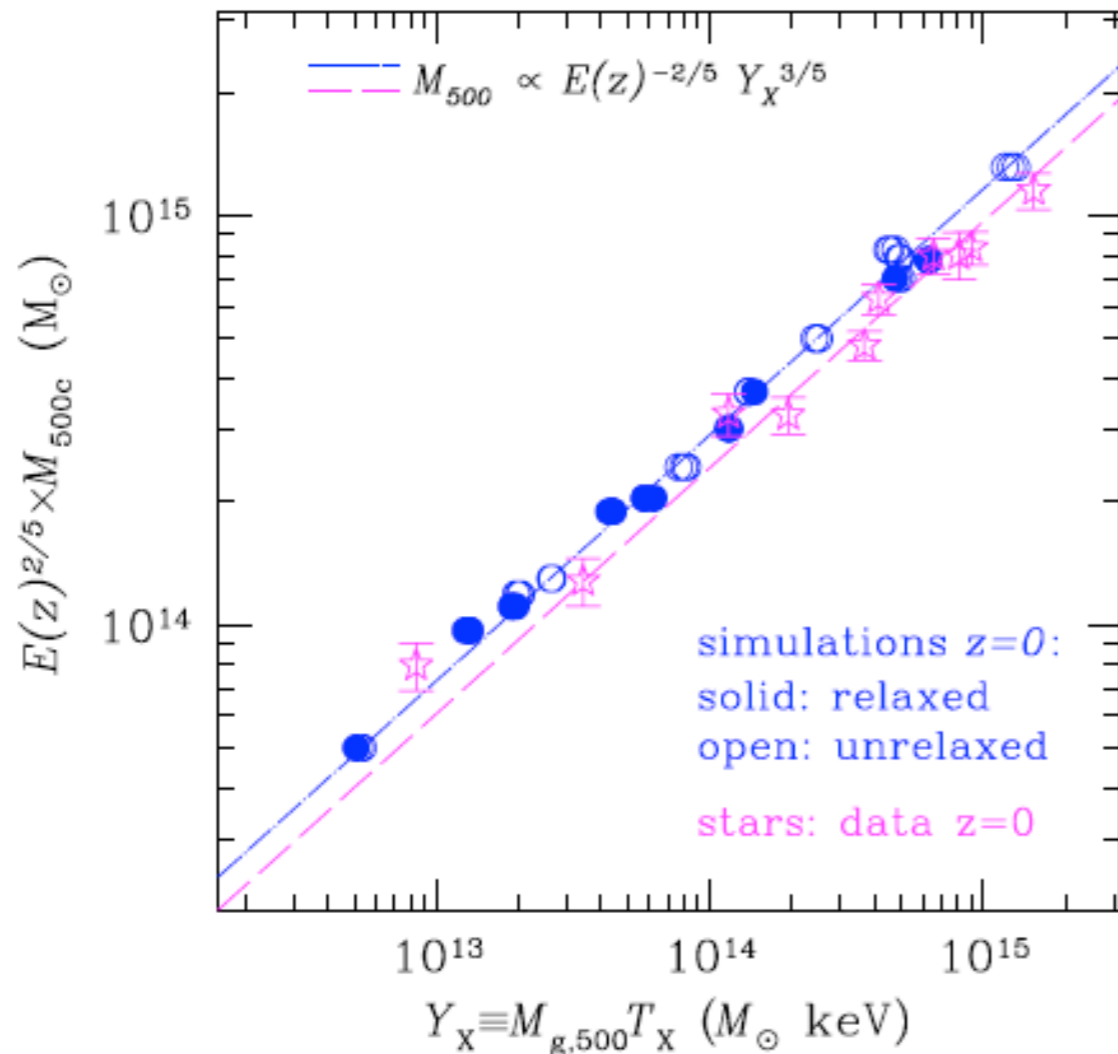
- bremsstrahlung emission

$$L_X \propto h(z) T^2$$



Observable - mass relations

Self-similar Mass- Y_X relation from simulations



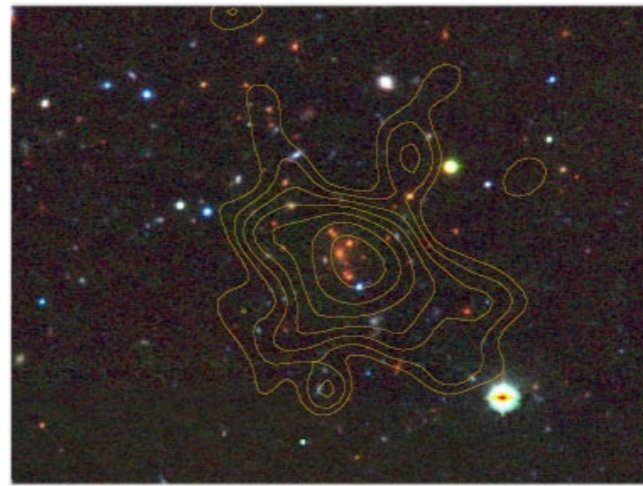
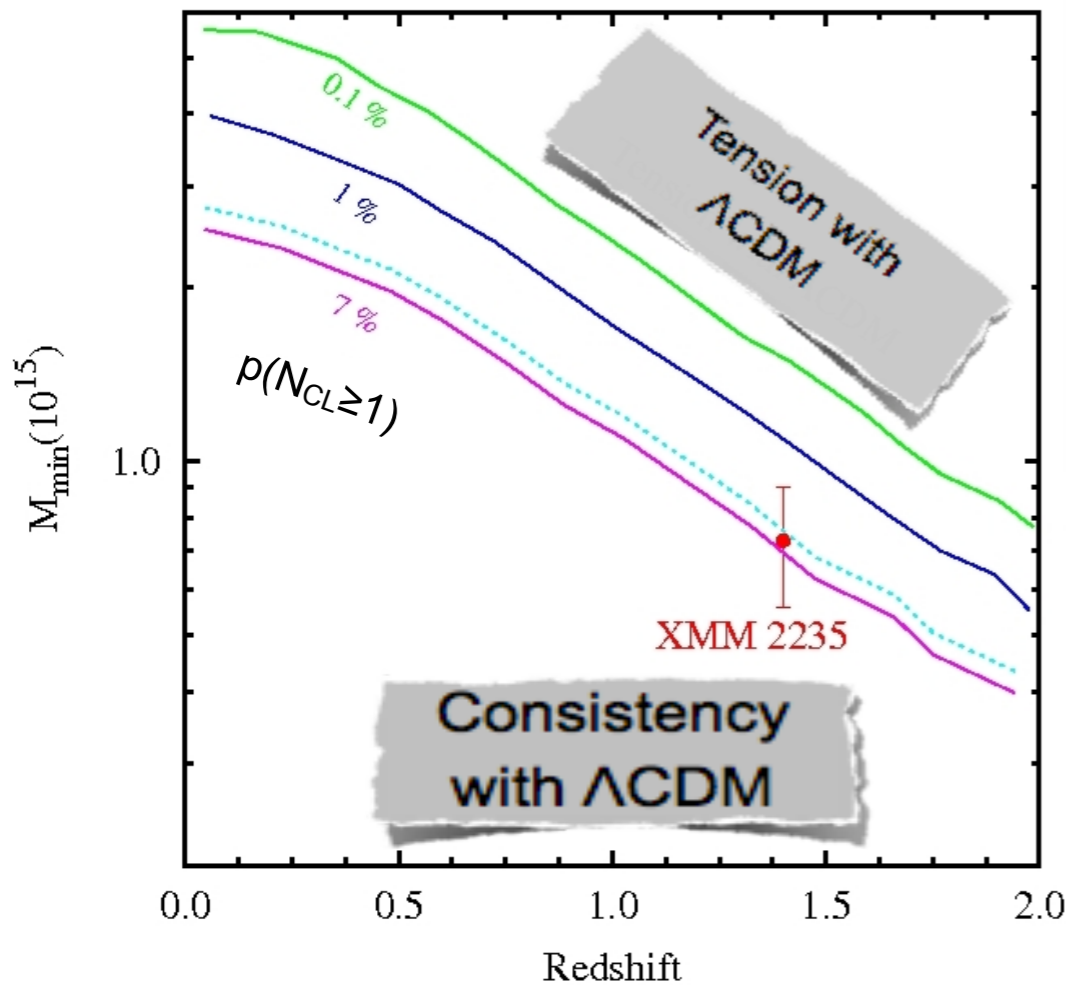
X-ray “pressure”:

$$Y_X = M_{\text{gas}} T_X$$

- Similar to Compton- y from SZ observations.
- Weaker sensitivity to ICM physics
- Always close to self-similar prediction
- Very small intrinsic scatter: $\sim 5-7\%$!
- About 15% offset wrt Chandra results.

Kravtsov, Nagai & Vikhlinin '06

The most massive distant clusters in the Universe and their impact on Cosmology



XMMU-J2235.3 cluster
(Jee et al. 2009) $z \sim 1.4$

Probability
of finding at least one
cluster with a given
redshift and mass

XDCP (50 deg² to 10^{-14} erg/cm²/s)

$$M_L = 7.3 \pm 1.7 \times 10^{14} M_{\odot} / h_{70}$$

Accurate (<10% errors) $M_{200,c}$ measurements needed

Sartoris et al. 2012 (in prep)

Parameters defining the mass - observable relations

number density of cluster

$$N_{l,m} = \Delta\Omega \int_{z_l}^{z_{l+1}} dz \frac{dV}{dzd\Omega} \int_{M_{l,m}^{ob}}^{M_{l,m+1}^{ob}} dM^{ob} \int_0^\infty dM n(M, z) p(M^{ob}||M) .$$

$$p(M_{ob}||M) = \frac{\exp[-x^2(M_{ob})]}{(2\pi\sigma_{\ln M}^2)^{1/2}}$$

Probability of assigning a mass M_{obs} to a cluster of “true” mass M :

$$x(M_{ob}) = \frac{\ln M_{ob} - B_M - \ln M}{(2\sigma_{\ln M}^2)^{1/2}}$$

B_M : intrinsic bias in mass estimates (e.g. violation of hydrostatic equilibrium)

$$\begin{aligned} B_M(z) &= B_{M,0}(1+z)^\alpha \\ \sigma_{\ln M}(z) &= \sigma_{\ln M,0}(1+z)^\beta \end{aligned}$$

4 “mass-parameters” :

$$B_{M,0}, \alpha, \sigma_{\ln M,0}, \beta$$

Constraints on cosmological parameters

Importance of mass accuracy

- Parameterize deviations from GR with:

$$\frac{d \ln \delta}{d \ln a} = \Omega_m(a)^\gamma$$

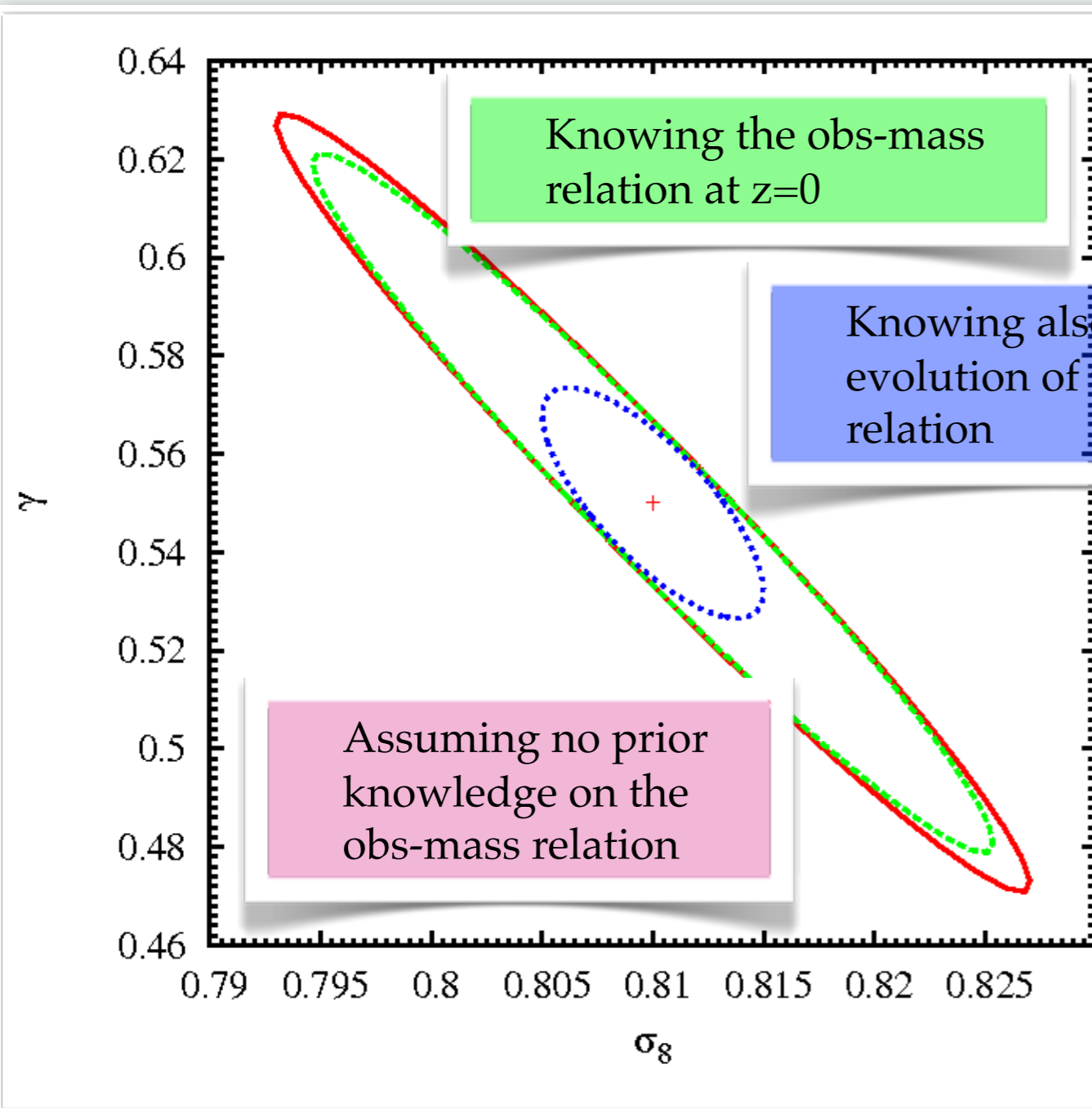
$\gamma=0.55$: standard GR

$\gamma=0.68$: DGP brane-world model

- Freeze expansion to Λ CDM and constrain dynamics: σ_8 and γ (Ω_m marginalized)

$$B_M(z) = B_{M,0}(1+z)^\alpha$$

$$\sigma_{\ln M}(z) = \sigma_{\ln M,0}(1+z)^\beta$$



The Fisher Matrix method

Fisher matrix:

$$F_{ij} \equiv - \left\langle \frac{\partial^2 \ln \mathcal{L}}{\partial p_i \partial p_j} \right\rangle$$

$$F_{\alpha\beta}^N = \sum_{l,m} \frac{\partial N_{l,m}}{\partial p_\alpha} \frac{\partial N_{l,m}}{\partial p_\beta} \frac{1}{N_{l,m}}$$

number density of cluster

+

$$F_{\alpha\beta} = \frac{1}{8\pi^2} \sum_{l,m,i} \frac{\partial \ln \bar{P}_{cl}(\mu_i, k_m, z_l)}{\partial p_\alpha} \frac{\partial \ln \bar{P}_{cl}(\mu_i, k_m, z_l)}{\partial p_\beta} V_{l,m,i}^{eff} k_m^2 \Delta k \Delta \mu$$

cluster power spectrum

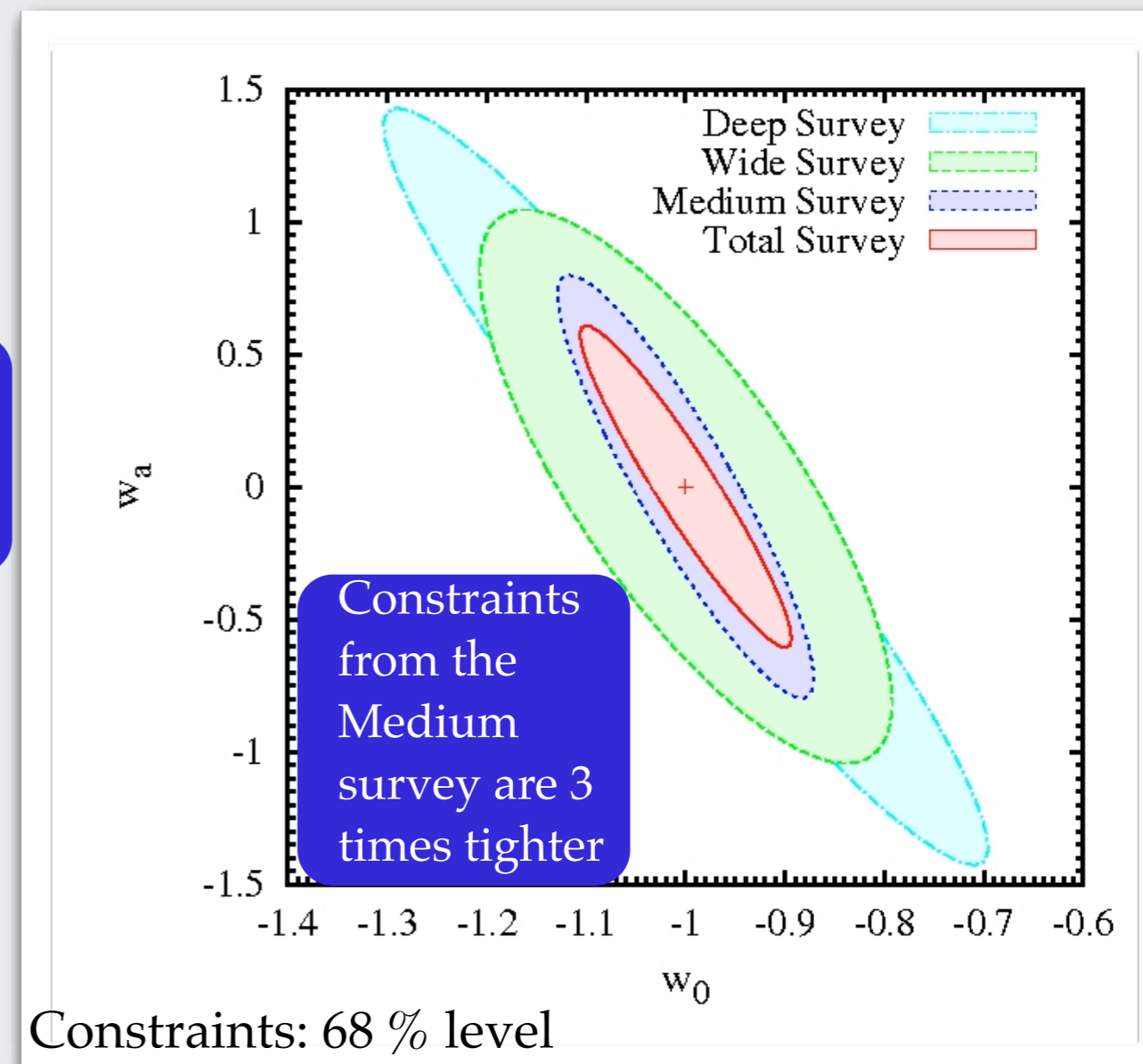
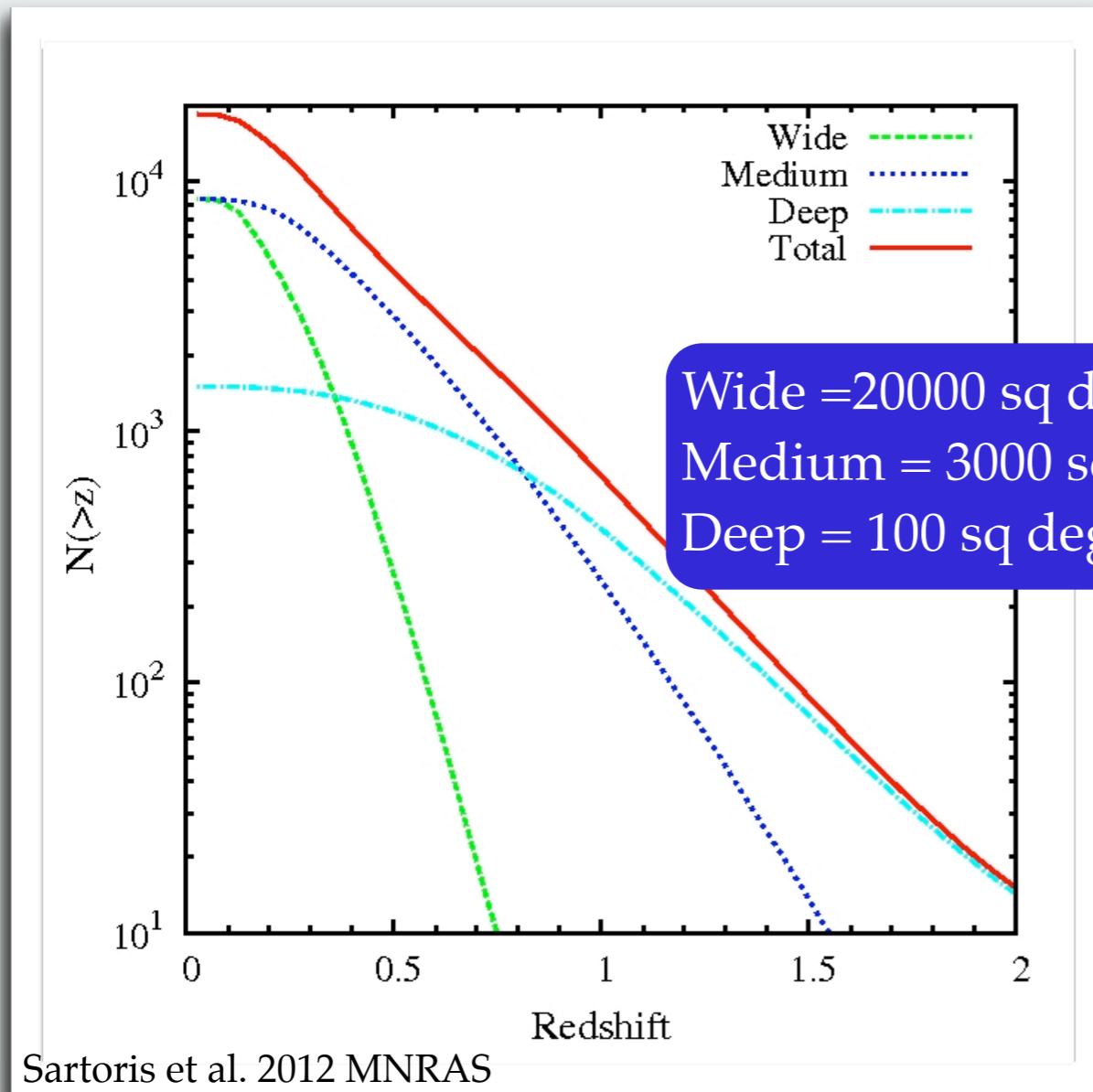
$$N_{l,m} = \Delta\Omega \int_{z_l}^{z_{l+1}} dz \frac{dV}{dz d\Omega} \int_{M_{l,m}^{ob}}^{M_{l,m+1}^{ob}} dM^{ob} \int_0^\infty dM n(M, z) p(M^{ob} \| M)$$

$$\bar{P}_{l,m,i}^{cl}(\mu, k, z_l) = \frac{\int_{z_l}^{z_{l+1}} dz \frac{dV}{dz} N^2(z) \tilde{P}_{damp}(\mu, k, z)}{\int_{z_l}^{z_{l+1}} dz \frac{dV}{dz} N^2(z)}$$

Survey redshift range

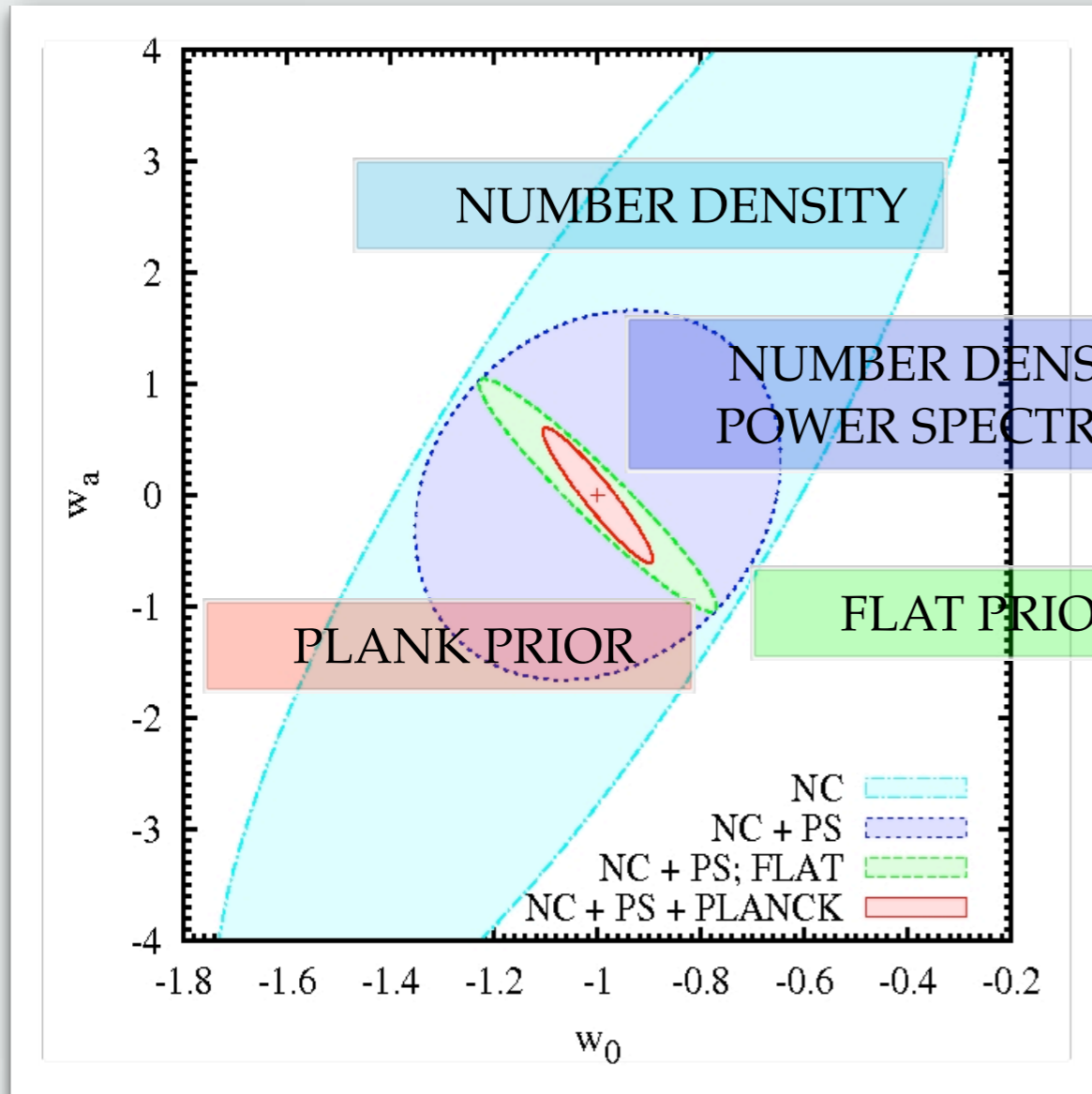
Cumulative redshift distribution

$$w(a) = w_0 + w_a(1 - a)$$



Constraints on cosmological parameters

Combining Cluster abundance and Power spectrum



$$w(a) = w_0 + w_a(1 - a)$$

$$\text{FoM}_{\text{DEFT}} = (\det [\text{Cov}(p_i, p_j)])^{-1/2}$$

Constraints: 68 % level

$$\Delta w_0 = 0.046$$

$$\Delta w_a = 0.14$$

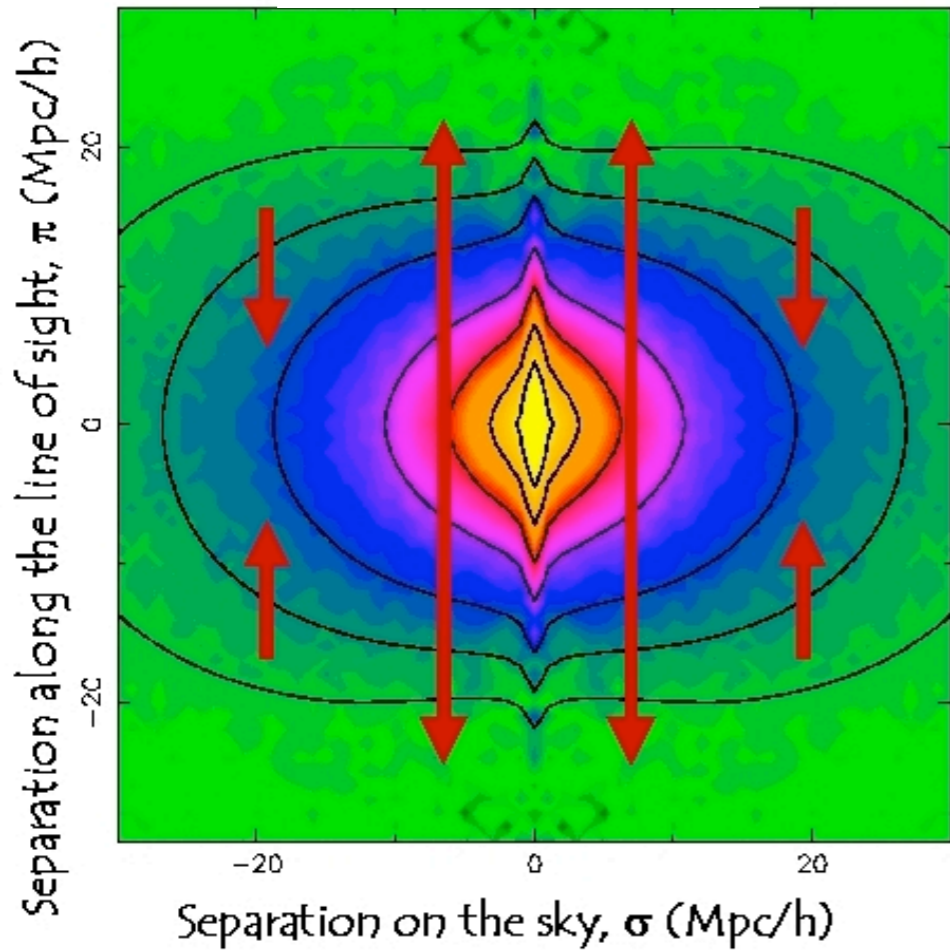
$$\text{FoM} = 106$$

Constraints on cosmological parameters from the Redshift Space Distortions

$$z_{\text{obs}} = z_{\text{true}} + v_{\text{pec}}/c \text{ where } v_{\text{pec}} \propto \Omega^{0.6} \delta\rho/\rho = (\Omega^{0.6}/b) \delta n/n$$

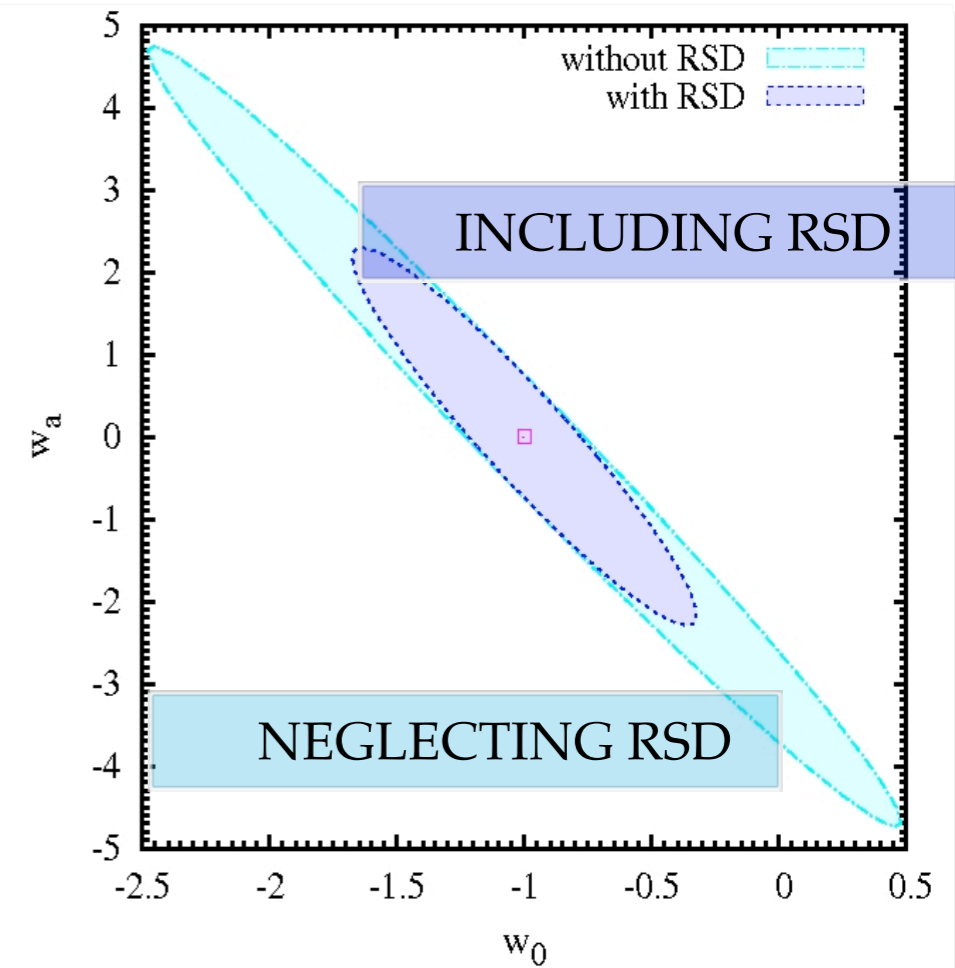
← bias

2gF galaxy catalogue



$$\tilde{P}(k, \mu) = (b + f\mu^2)^2 P(k)$$

$$f = \frac{d \ln D}{d \ln a}$$

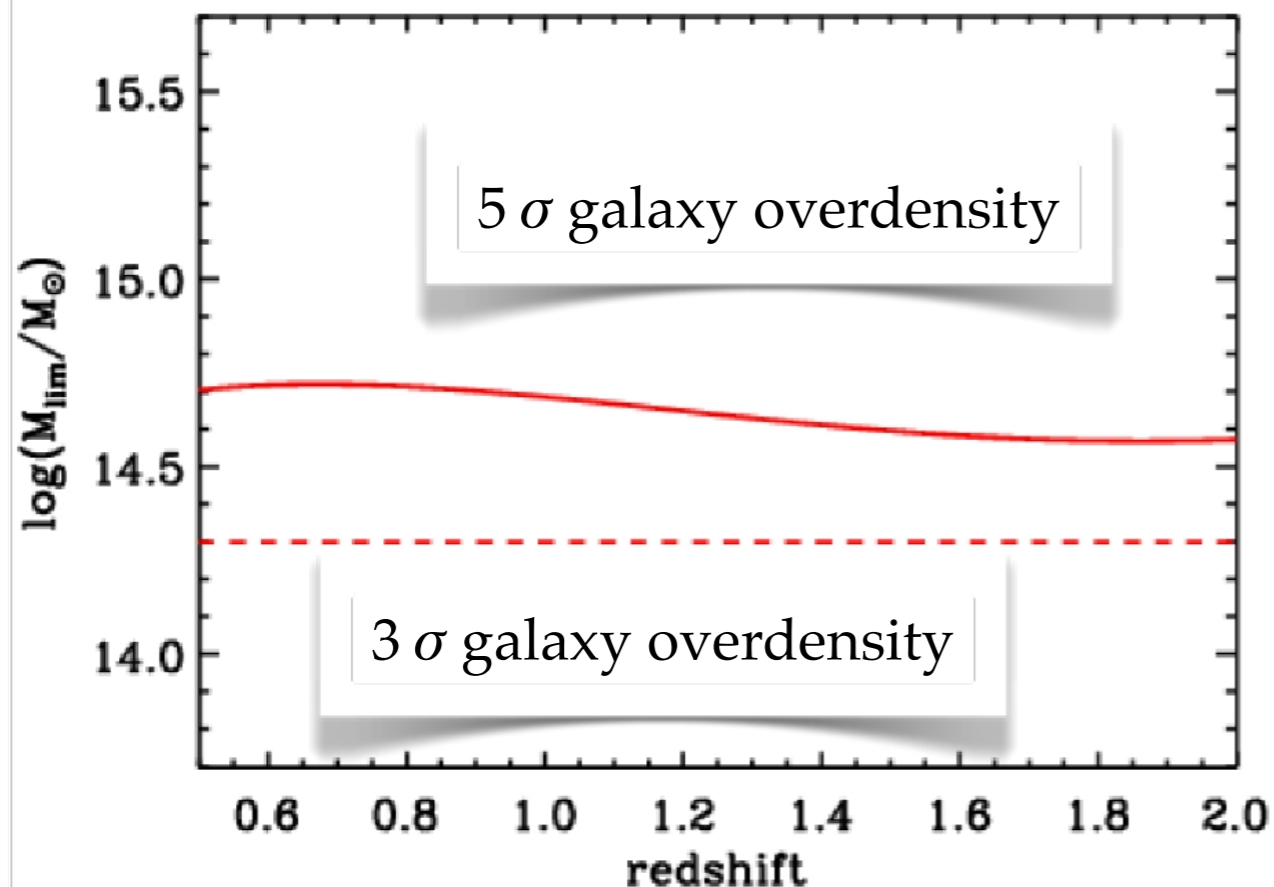


$$\text{FoM}_{\text{RSD}} / \text{FoM}_{\text{noRSD}} = 2$$

Sartoris et al. 2012 MNRAS

Constraints at 68 % level

DE forecast from future optical near-IR Euclid survey



Mission approved by ESA with the primary aim to study the origin of the Universe expansion (measure of w) from BAO+WL cosmic shear

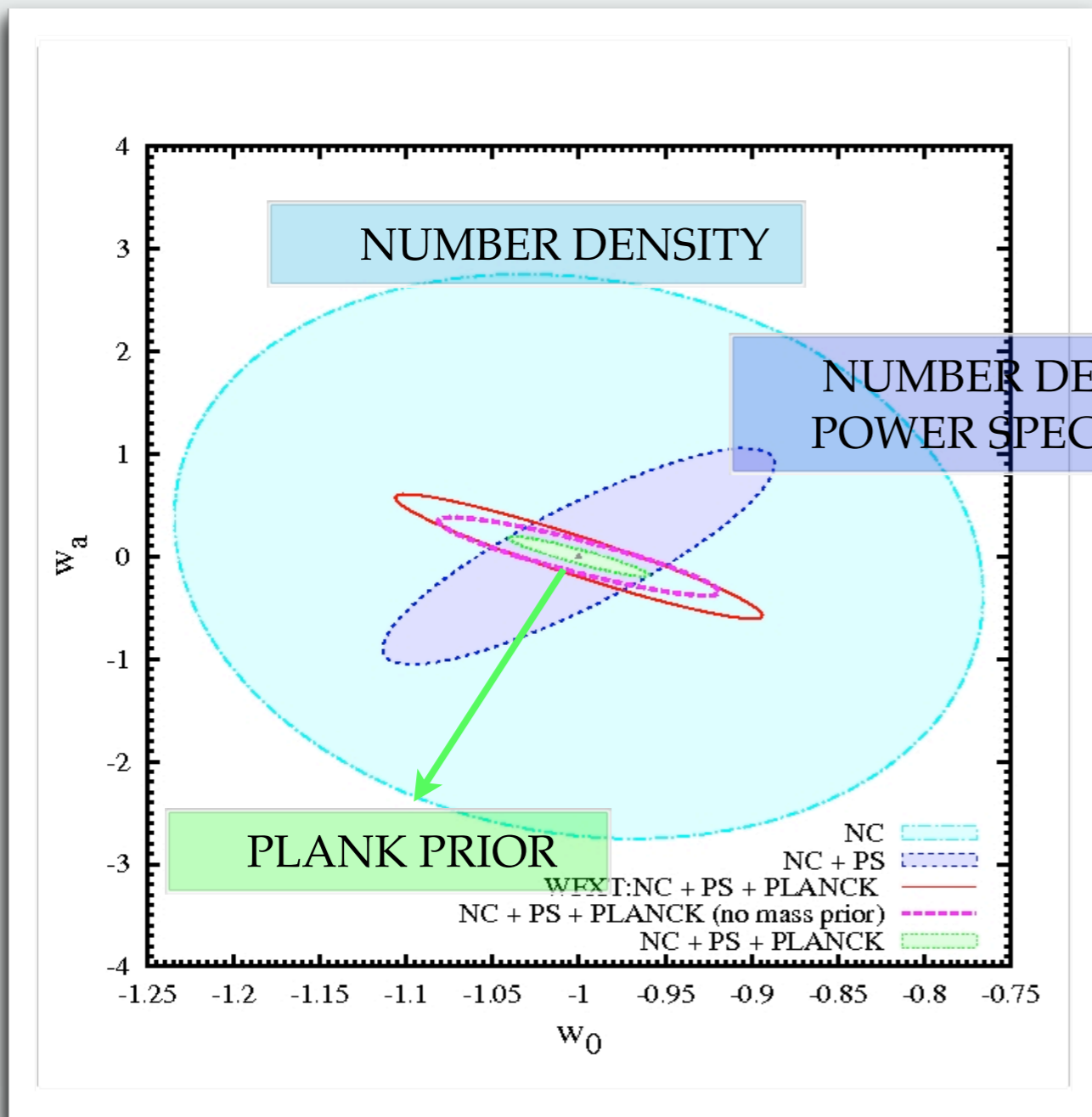
- optical band: 550- 900 nm with a resolution of <0.2 arcsec
- NIR band: 920-2000 nm

Combination with ground experiments Pan-STARRS and LSST.

20000 sq deg.

Euclid cluster sample: 3000 clusters detected via photometry with WL mass measurements.

DE forecast from future optical near-IR Euclid survey



Mission approved by ESA with the primary aim to study the origin of the Universe expansion (measure of w) from BAO+WL cosmic shear

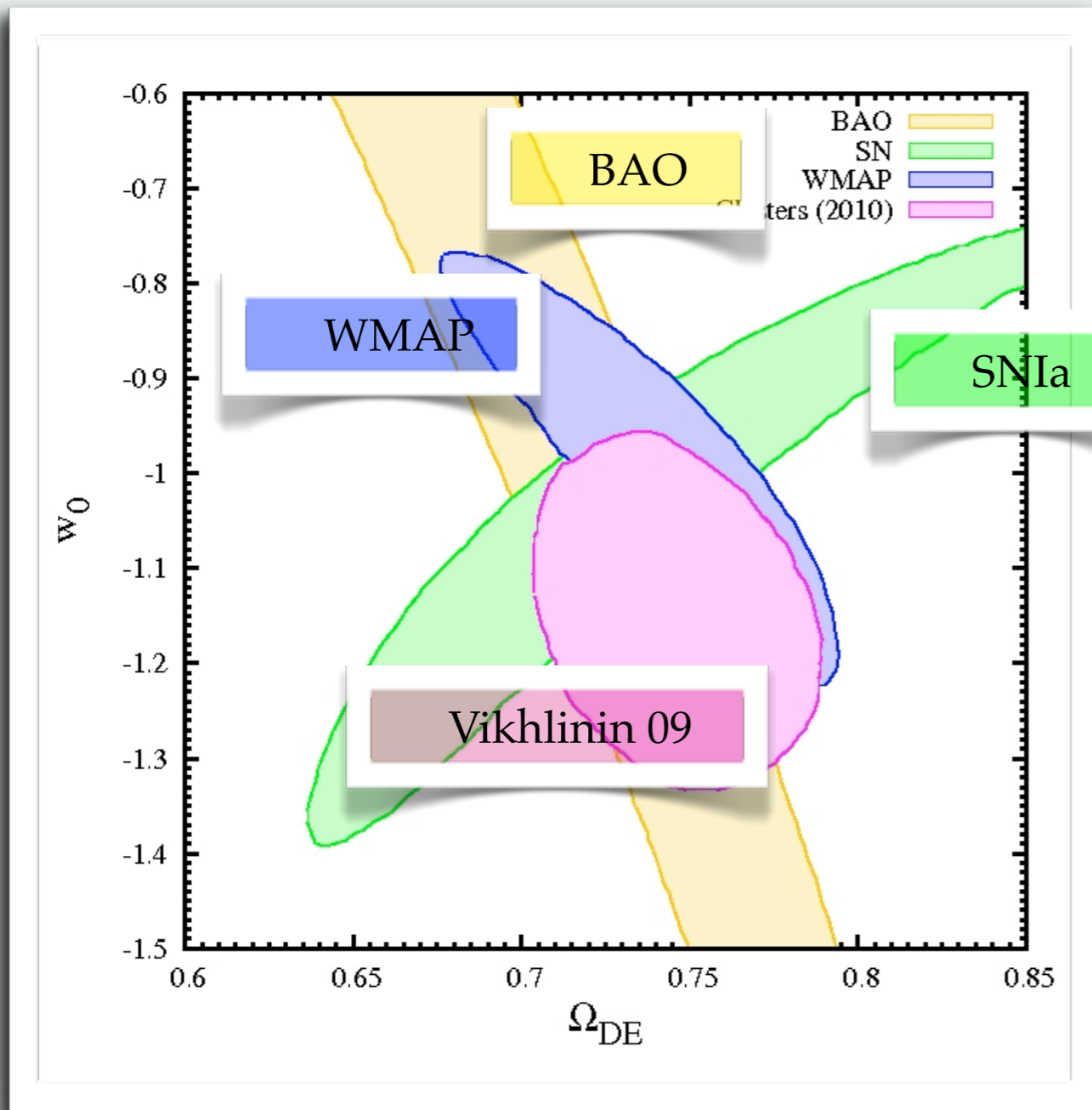
- optical band: 550- 900 nm with a resolution of <0.2 arcsec
- NIR band: 920-2000 nm

Combination with ground experiments Pan-STARRS and LSST.

20000 sq deg.

Euclid cluster sample: 30000 clusters detected via photometry with WL mass measurements.

Dark Energy constraints from clusters current data



→ Flat universe

→ Constant DE EoS

● Constraints from galaxy clusters:

$$w_0 = -1.1 \pm 0.2$$

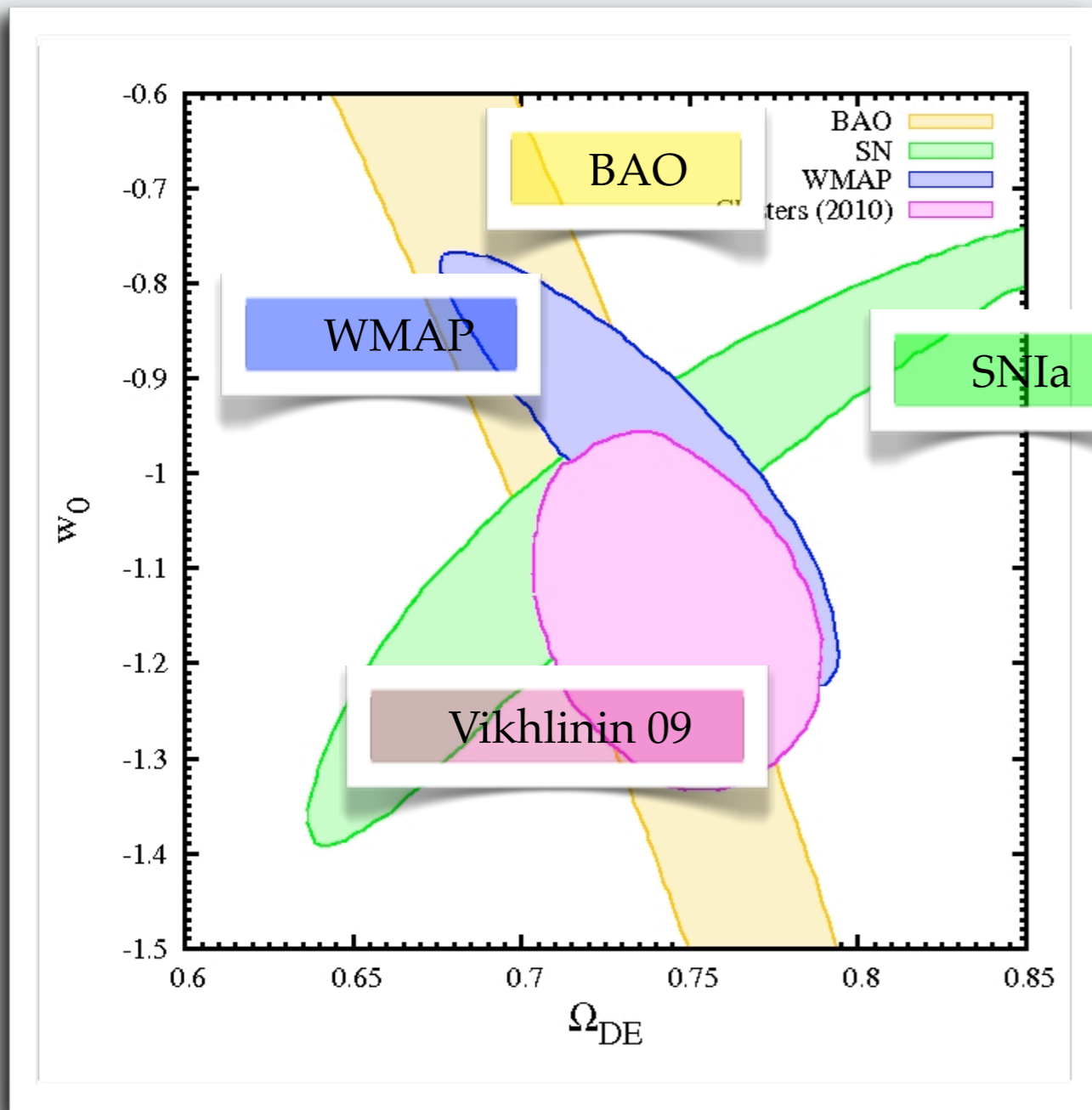
$$\Omega_{DE} = 0.75 \pm 0.04$$

● Joint constraints:

$$w_0 = -0.99 \pm 0.05$$

$$\Omega_{DE} = 0.74 \pm 0.02$$

Dark Energy constraints from clusters current data

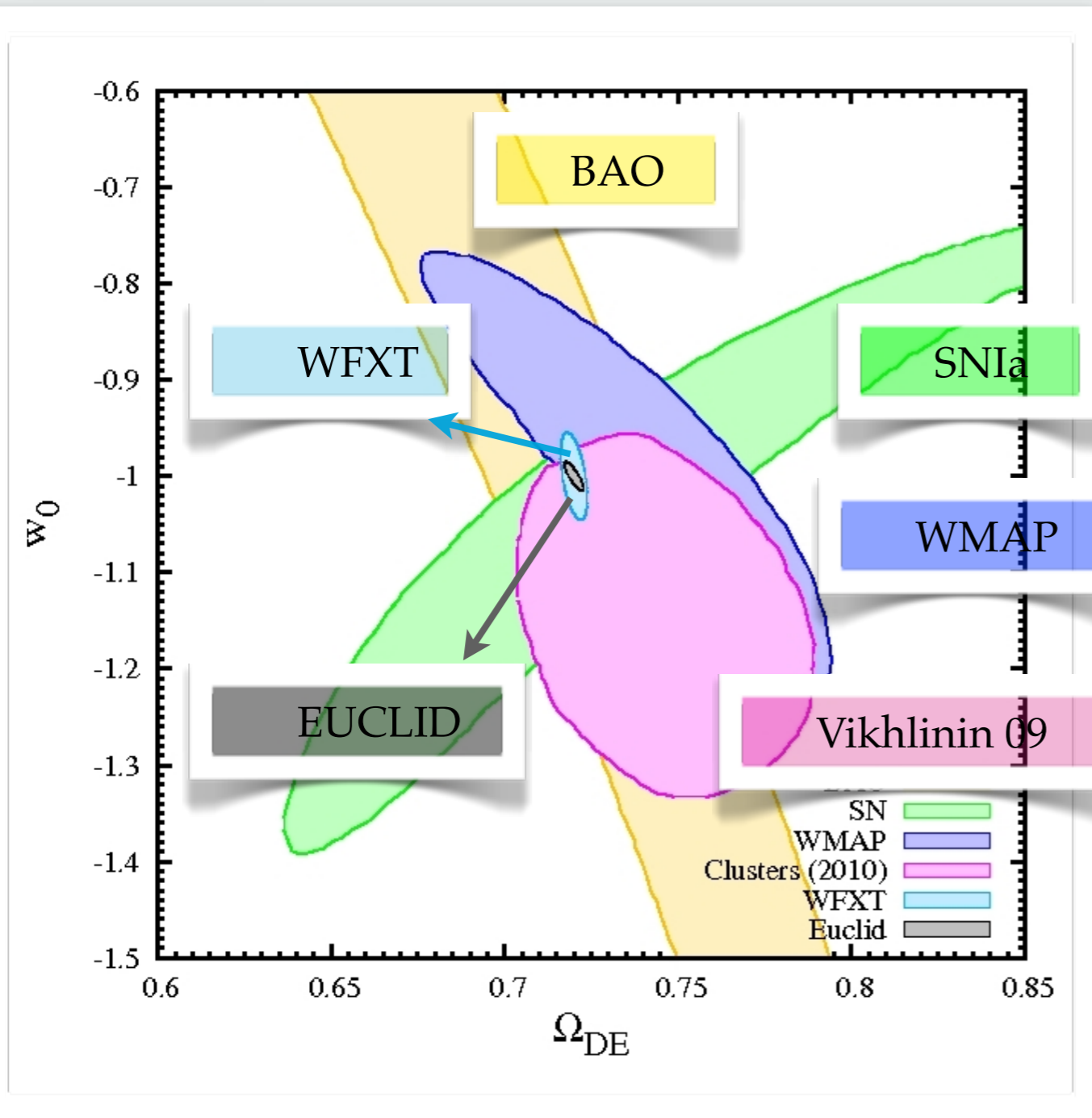


Constraints from clusters number density obtained with:

- 49 brightest clusters at $z \approx 0.05$ detected in the X-ray ROSAT All-Sky Survey
- 37 clusters ($\langle z \rangle = 0.55$) derived from 400 sq. Deg. X-ray ROSAT serendipitous survey

Follow up observations of all clusters with Chandra.

Dark Energy constraints from clusters current and future survey



→ Flat universe

→ Constant DE EoS

● Constraints from clusters (2010):

$$w = -1.1 \pm 0.2$$

$$\Omega_{DE} = 0.75 \pm 0.04$$

● Constraints from EUCLID:

more than one order of magnitude tighter.

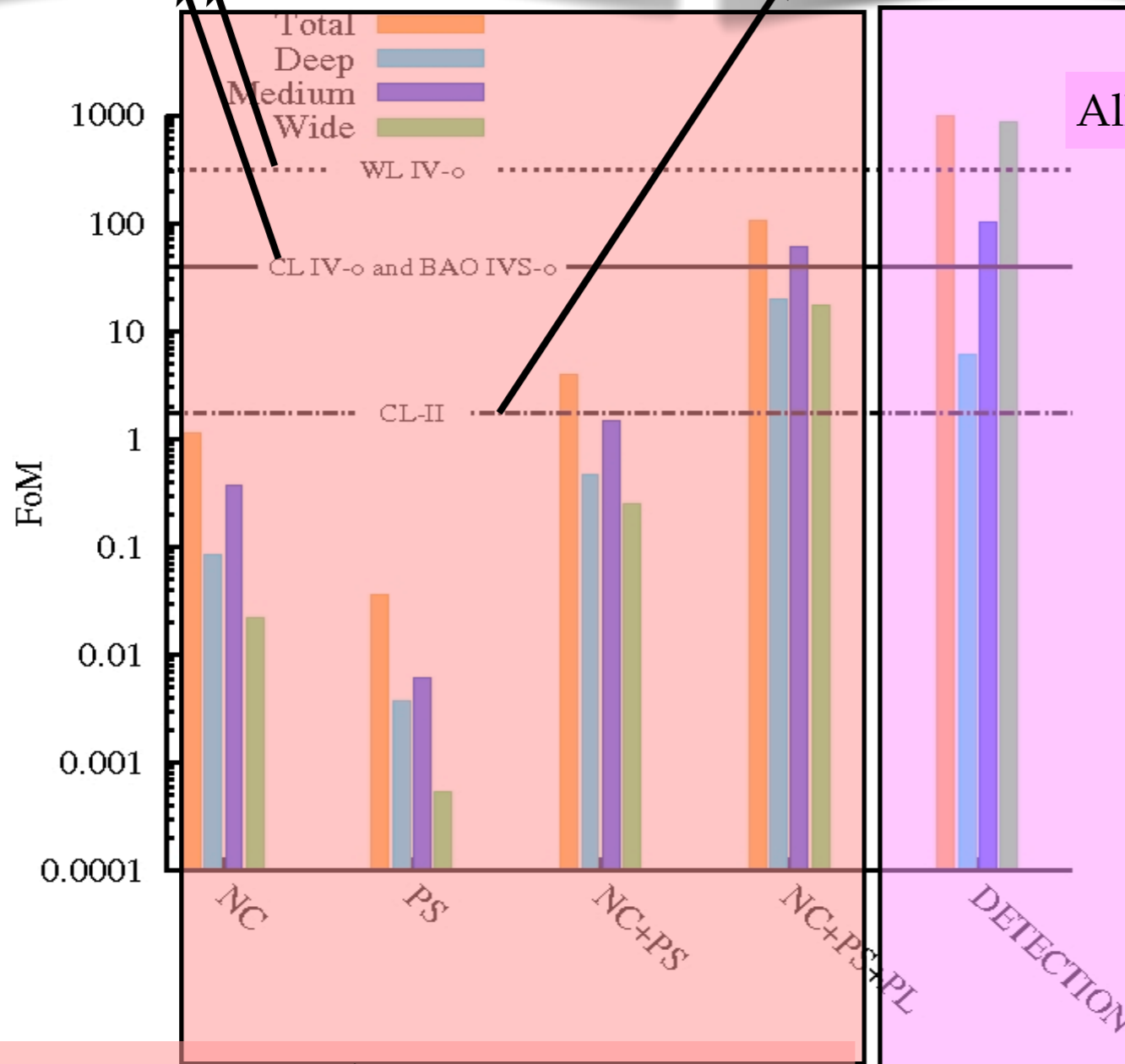
Constraints at 68 % level

Dark Energy Task Force FoM

Future Cluster, BAO and WL surveys

Current Cluster surveys

$$FoM_{DEFT} = (\det [Cov(p_i, p_j)])^{-1/2}$$



All WFXT clusters

$$w(a) = w_0 + w_a(1 - a)$$

Constraints from 2×10^4 WXFT clusters with direct mass measurements:

$$\Delta w_0 = 0.046$$

$$\Delta w_a = 0.14$$

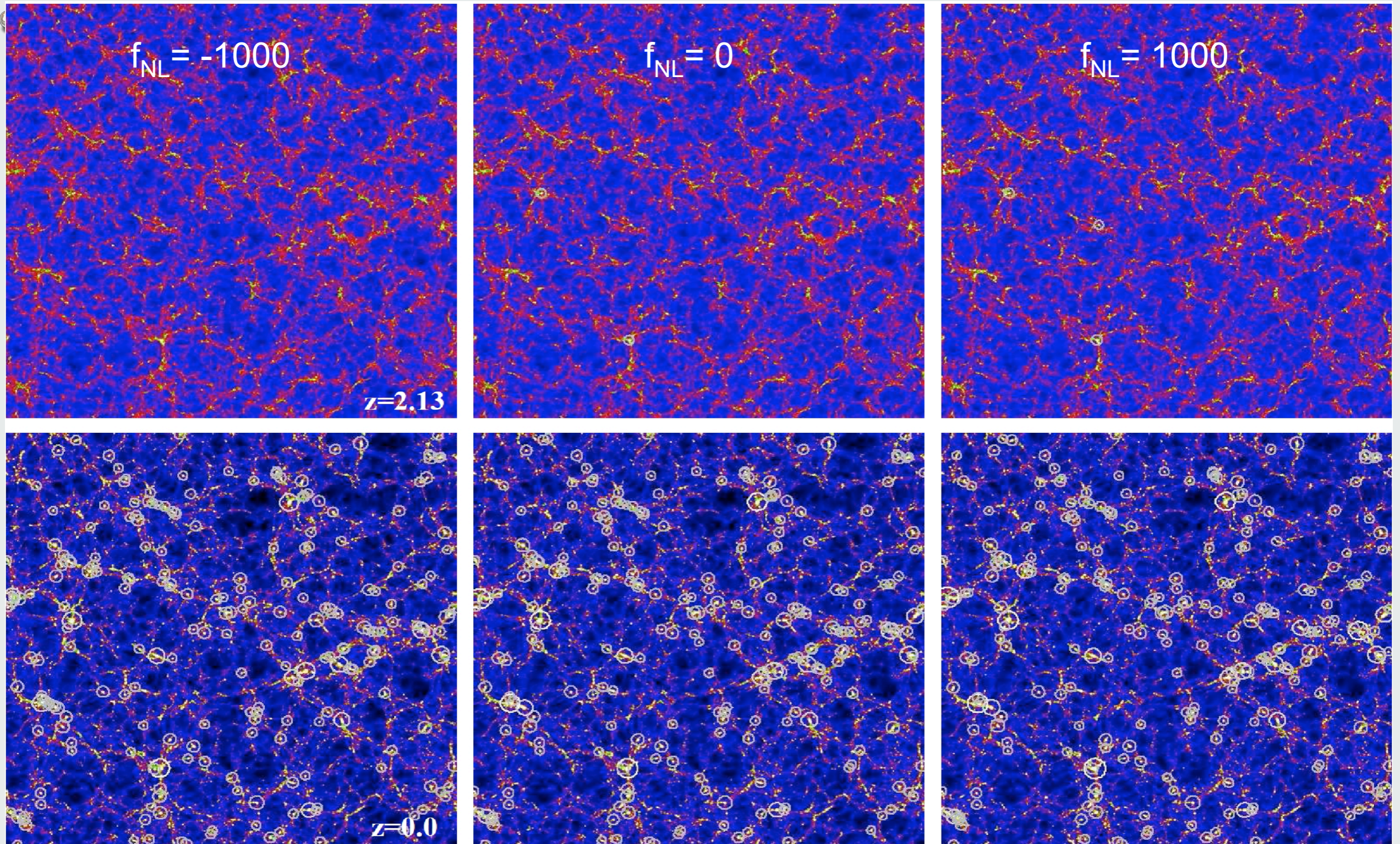
$$FoM = 106$$

WXFT Clusters with mass measurements

Sartoris et al. 2012 MNRAS

Non-Gaussian evolution of clusters

Grossi et al. 2007



Non Gaussian initial conditions

- Parametrize deviations from Gaussian initial fluctuations:

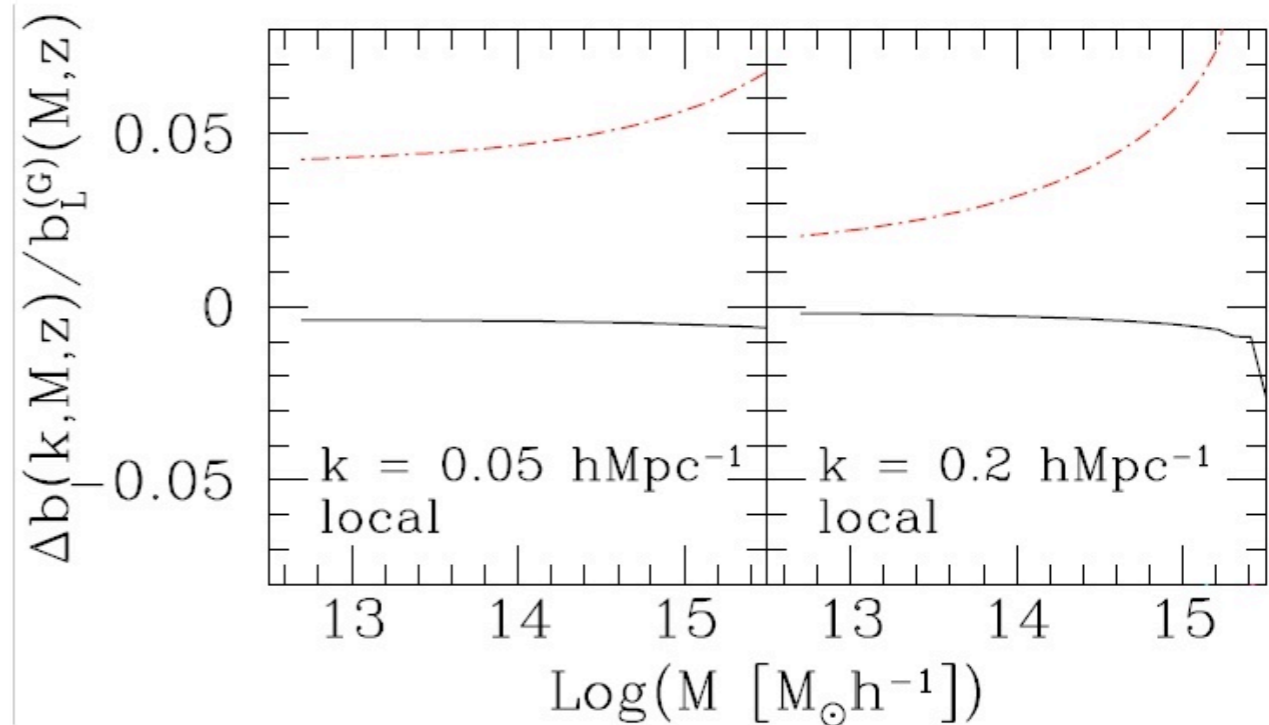
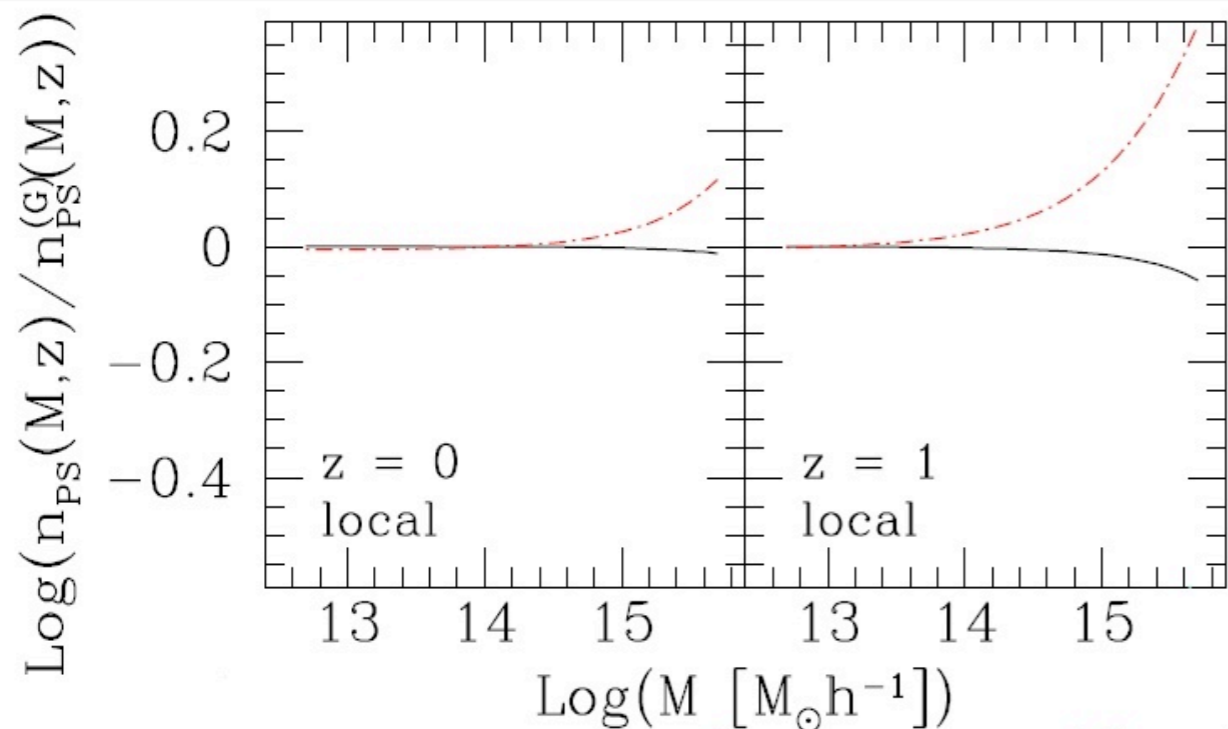
$$\Phi = \Phi_G + f_{\text{NL}} * (\Phi_G^2 - \langle \Phi_G^2 \rangle)$$

$f_{\text{NL}}=0$ standard cosmology

Positive skewness: collapse of halos at higher z , for fixed σ_8 .

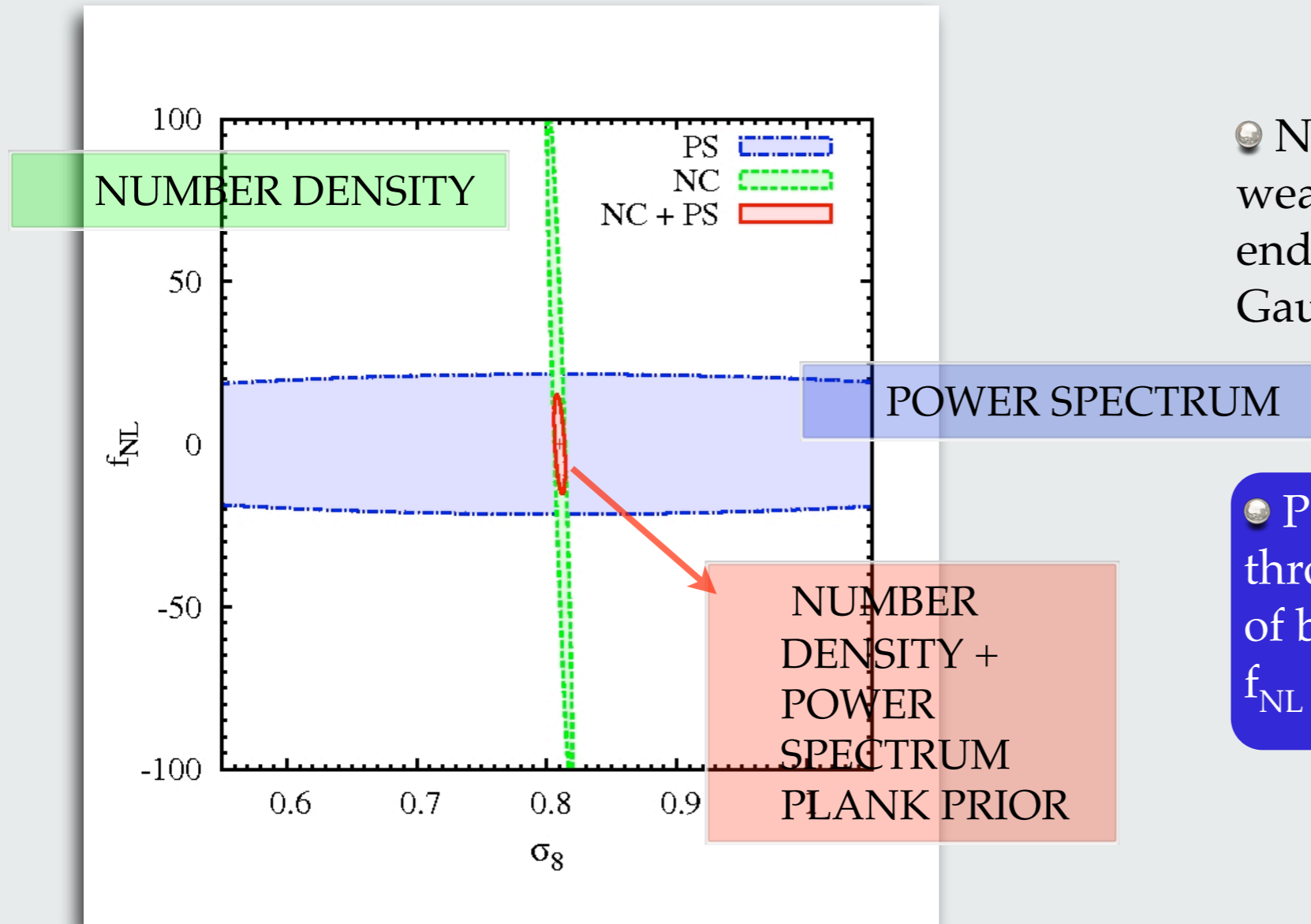
$$n(M, z) = n^{(\text{G})}(M, z) \frac{n_{\text{PS}}(M, z)}{n_{\text{PS}}^{(\text{G})}(M, z)}$$

$$b(M, z, k) = 1 + b_L^{(\text{G})}(M, z) \left[1 + \frac{\Delta b(M, z, k)}{b_L^{(\text{G})}(M, z)} \right]$$



Constraints on Non-Gaussianity

Strong complementarity NC and PS to constrain σ_8 and f_{NL} .



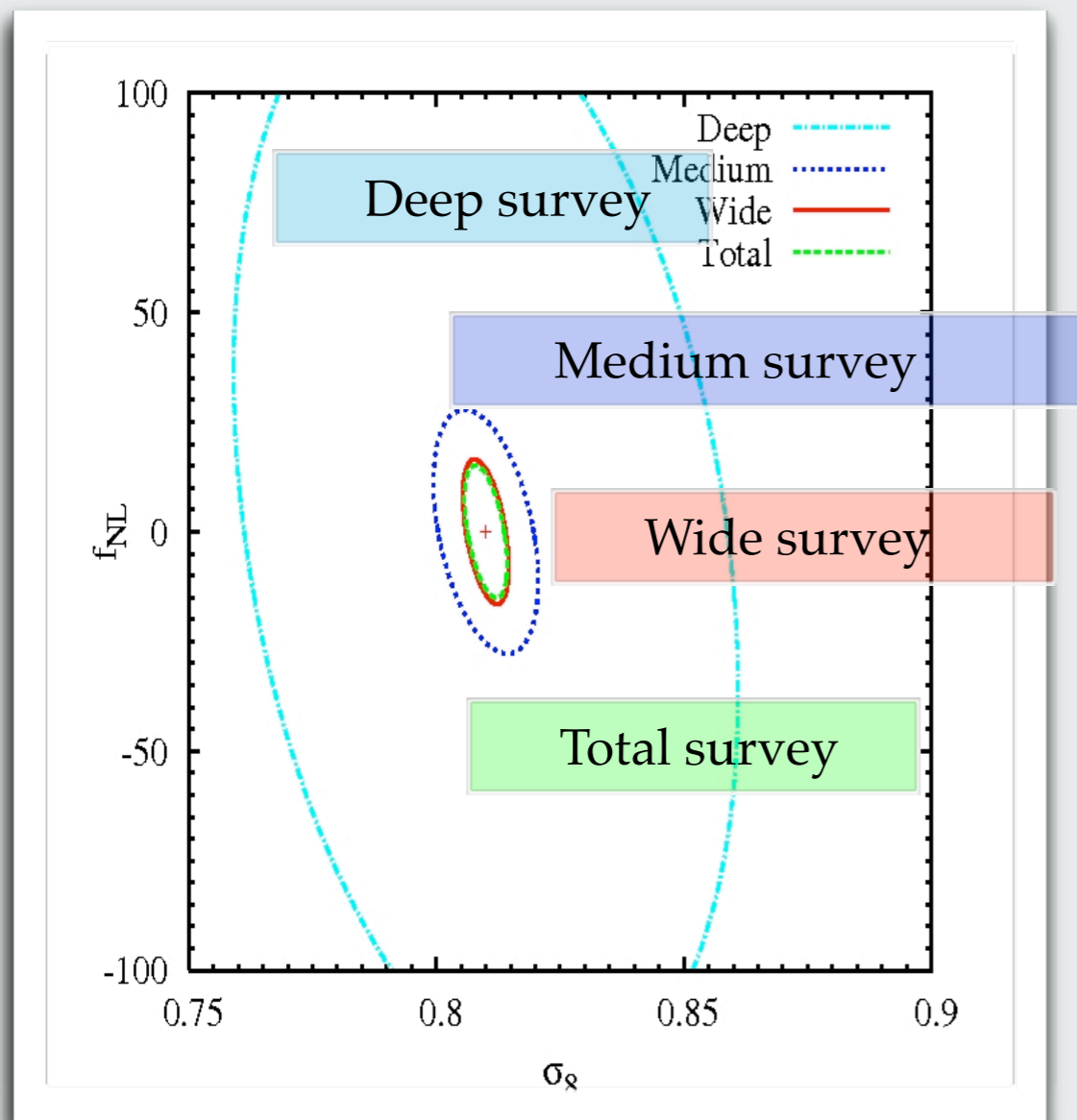
● Number Counts:
weakly sensitive of the high
end of the mass function to non
Gaussianity and so on f_{NL} .

● Power Spectrum:
through the scale-dependence
of bias strong constraints on
 f_{NL}

Constraints at 68 % level

Constraints on Non-Gaussianity

Combine all the information obtainable from the three WXFXT surveys



Most of the constraining power from Wide survey:

➔ larger statistics out to $z \approx 1$

➔ better sample long-wavelength modes

● Constraints from WFXT:
 $\Delta f_{NL} \approx 12$

● Current constraints from CMB (WMAP-7):

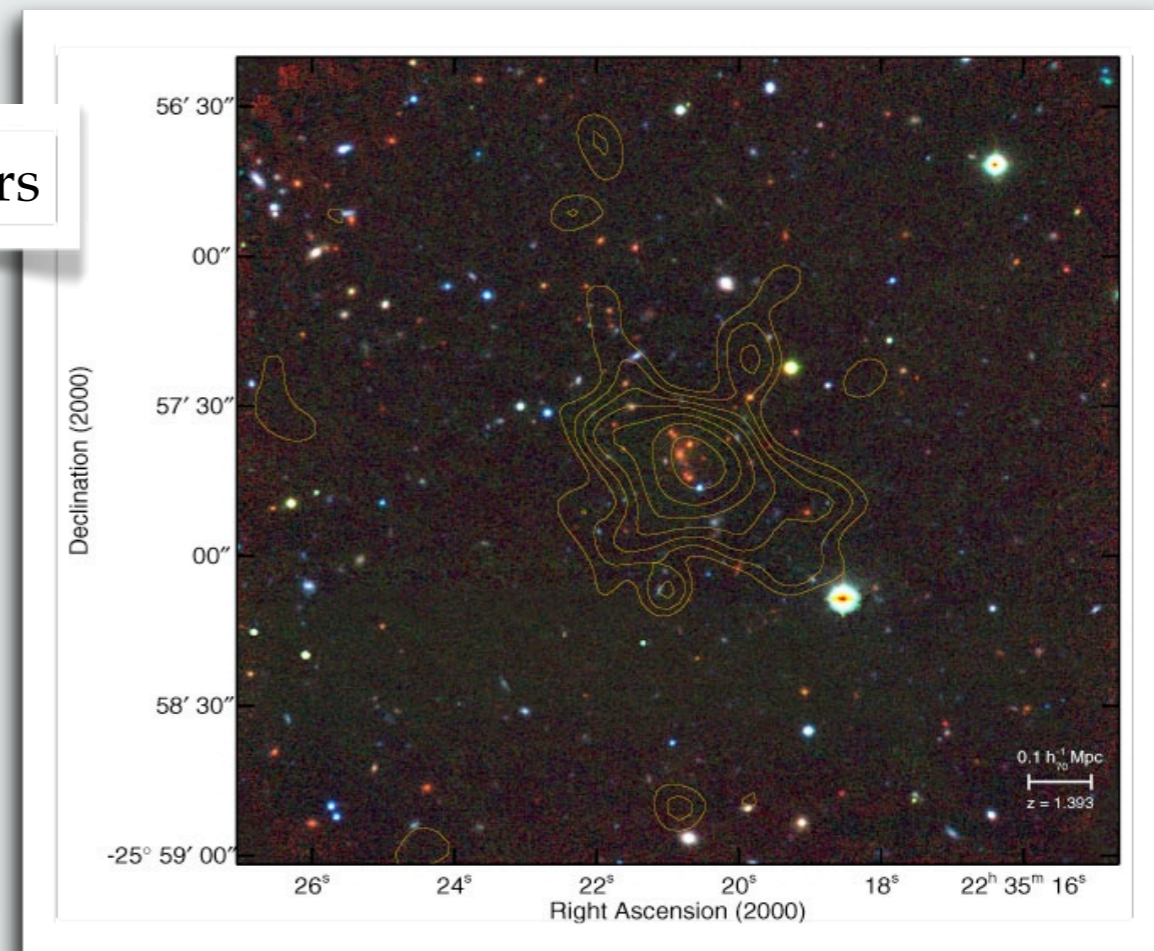
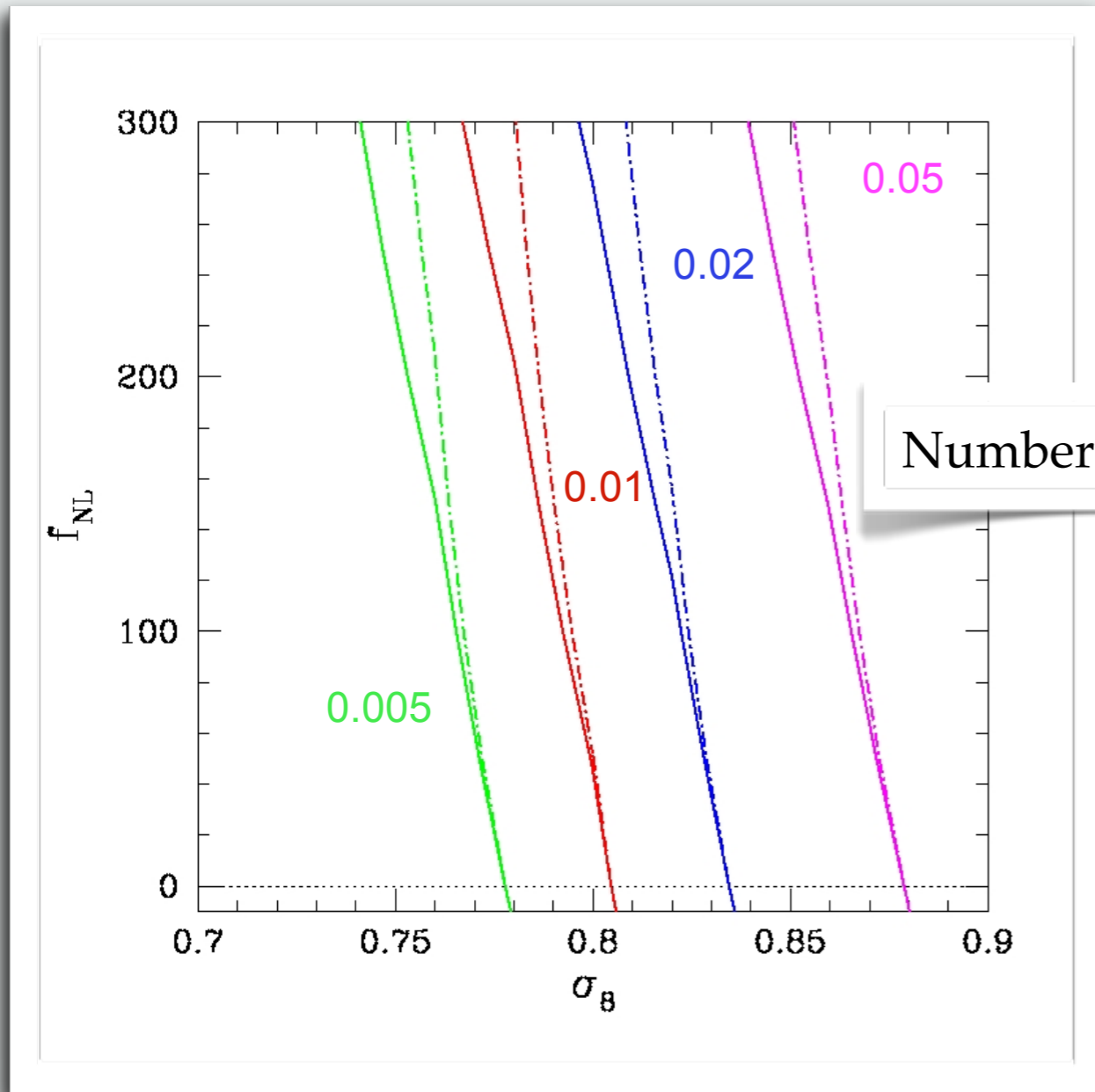
$-9 < f_{NL}^{CMB} < 111$ (95% C.L.)
(Komatsu et al. 09)

Constraints at 68 % level

Using high-z massive clusters to constrain Non-Gaussianity

XMMU-J2235.3 cluster (Jee et al. 2009) $z \sim 1.4$, $M = 5 \times 10^{14} M_{\odot}$ detected in 11 sq.deg.

Number of clusters with mass $M > 5 \times 10^{14} M_{\odot}$, found in the redshift range $1.4 < z < 2$ within 11 sq.deg.



Sartoris et al. 2010 MNRAS 407,2339

Mullis et al. 2005, Jee et al. 2009

Cosmology with clusters of galaxies

Galaxy clusters as cosmological probes

Growth tests

Geometrical tests

Forecasts from future surveys

The importance of the observable mass calibration

Combination of power

spectrum and number density

Dark Energy constraints

Non Gaussian constraints

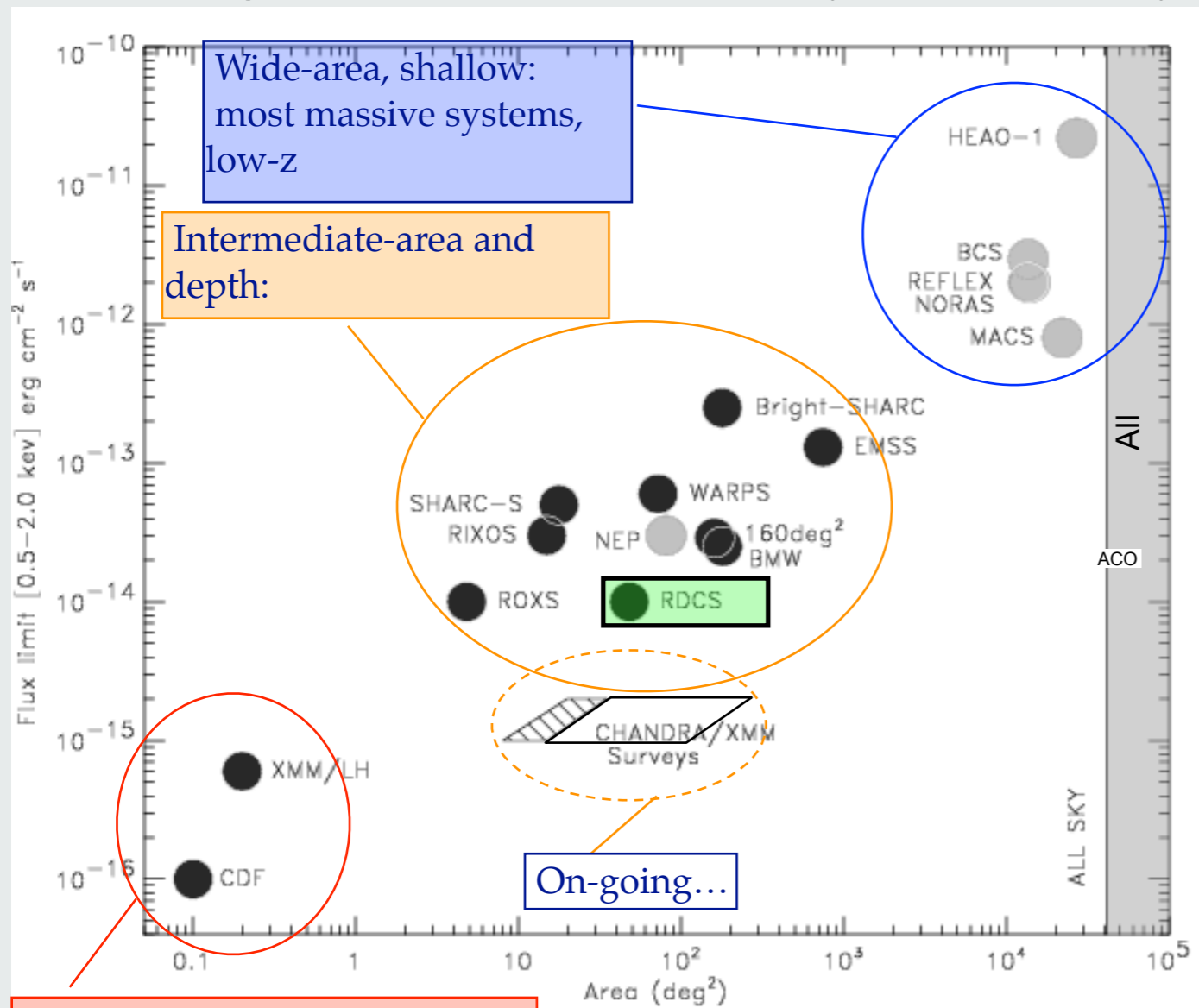
Cosmological constraints from current cluster surveys

Massive high-redshift clusters

High-redshift ($z > 0.8$) mass function

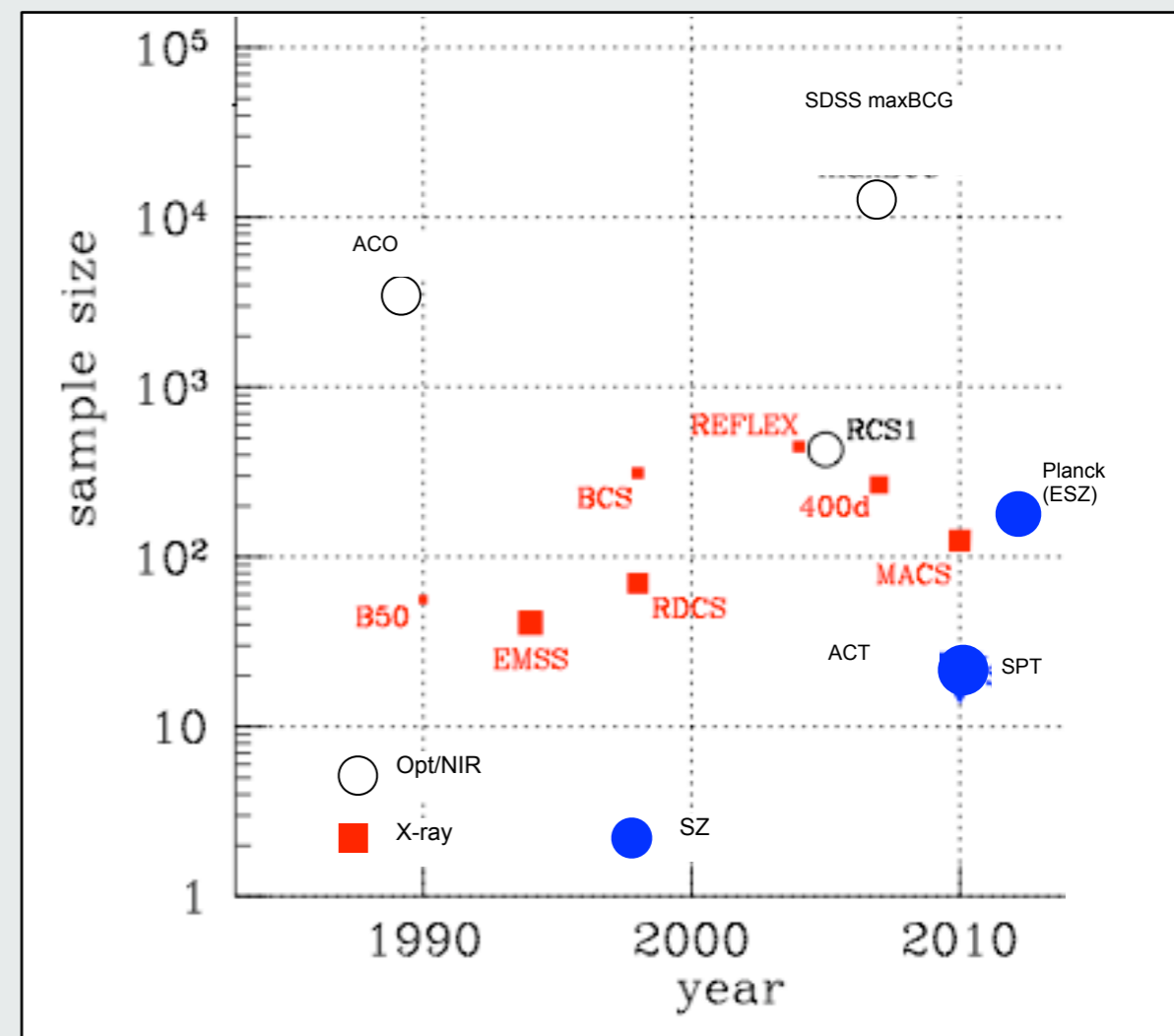
Cluster Surveys (1980 - 2010)

Solid angles and flux limits of X-ray cluster surveys

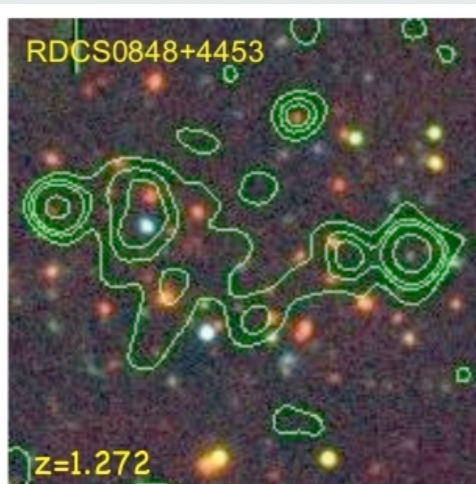
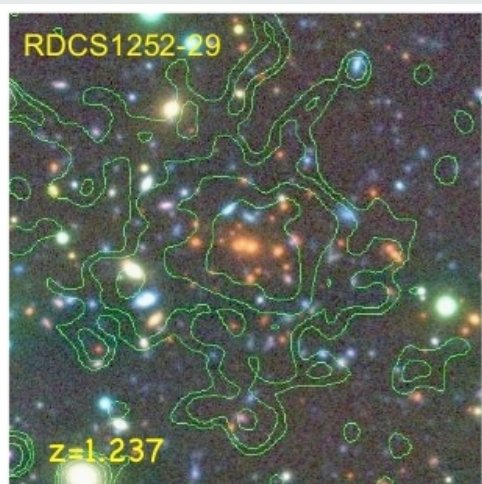


In order to obtain tight constraints we need :

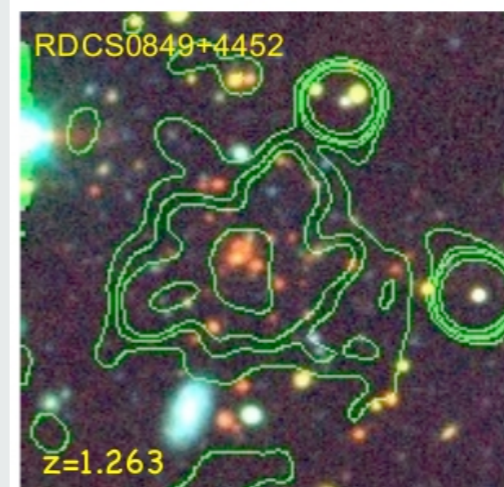
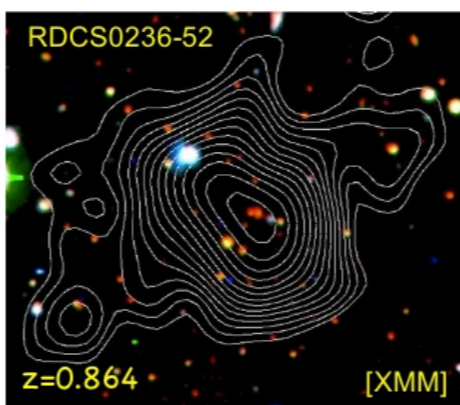
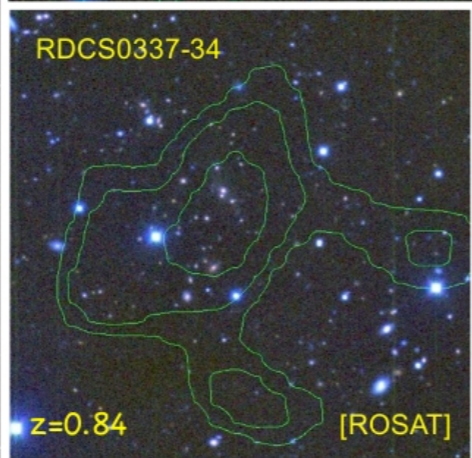
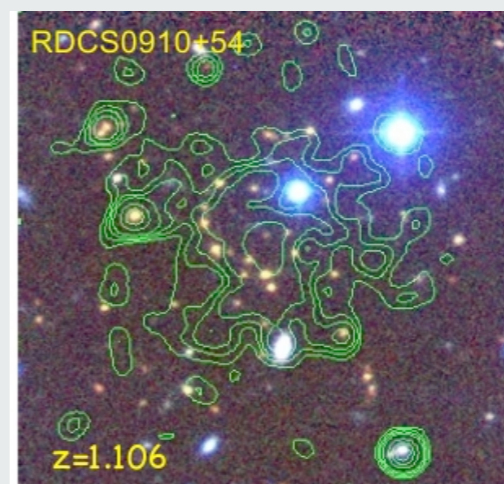
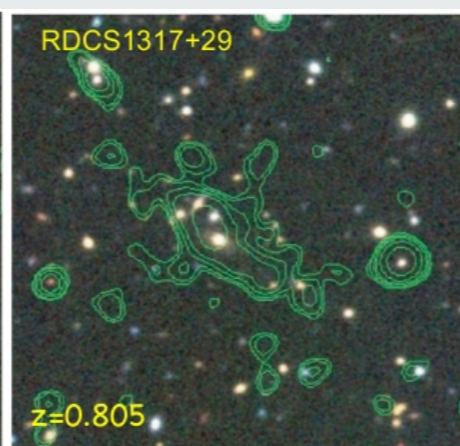
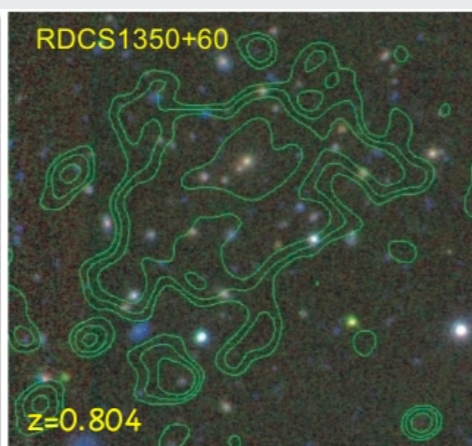
- a robust measurement of the mass proxies
- a large statistic of clusters (especially at high redshifts)



ROSAT Deep Cluster Sample - RDCS



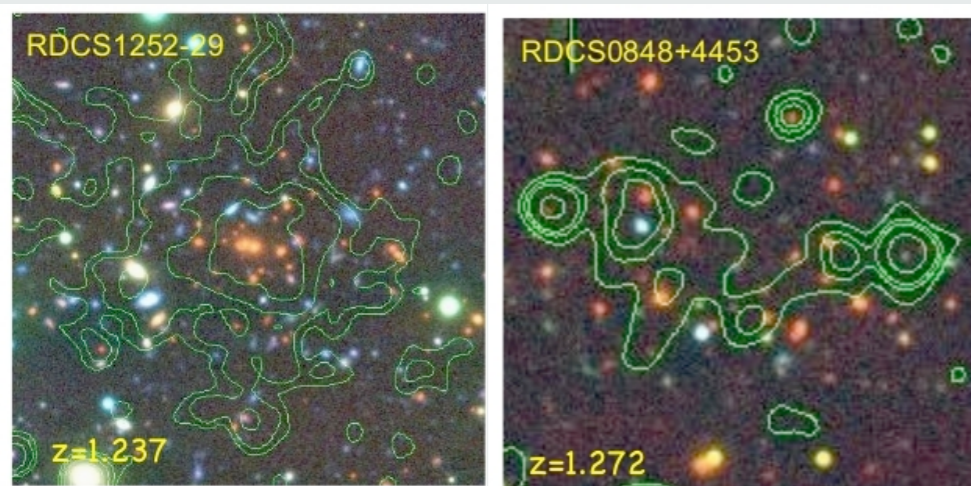
RDCS high-z sample
($f_{\text{lim}} = 10^{-14}$ erg/cm²/s
[0.5 – 2]keV band)
 $0.8 < z < 1.3$



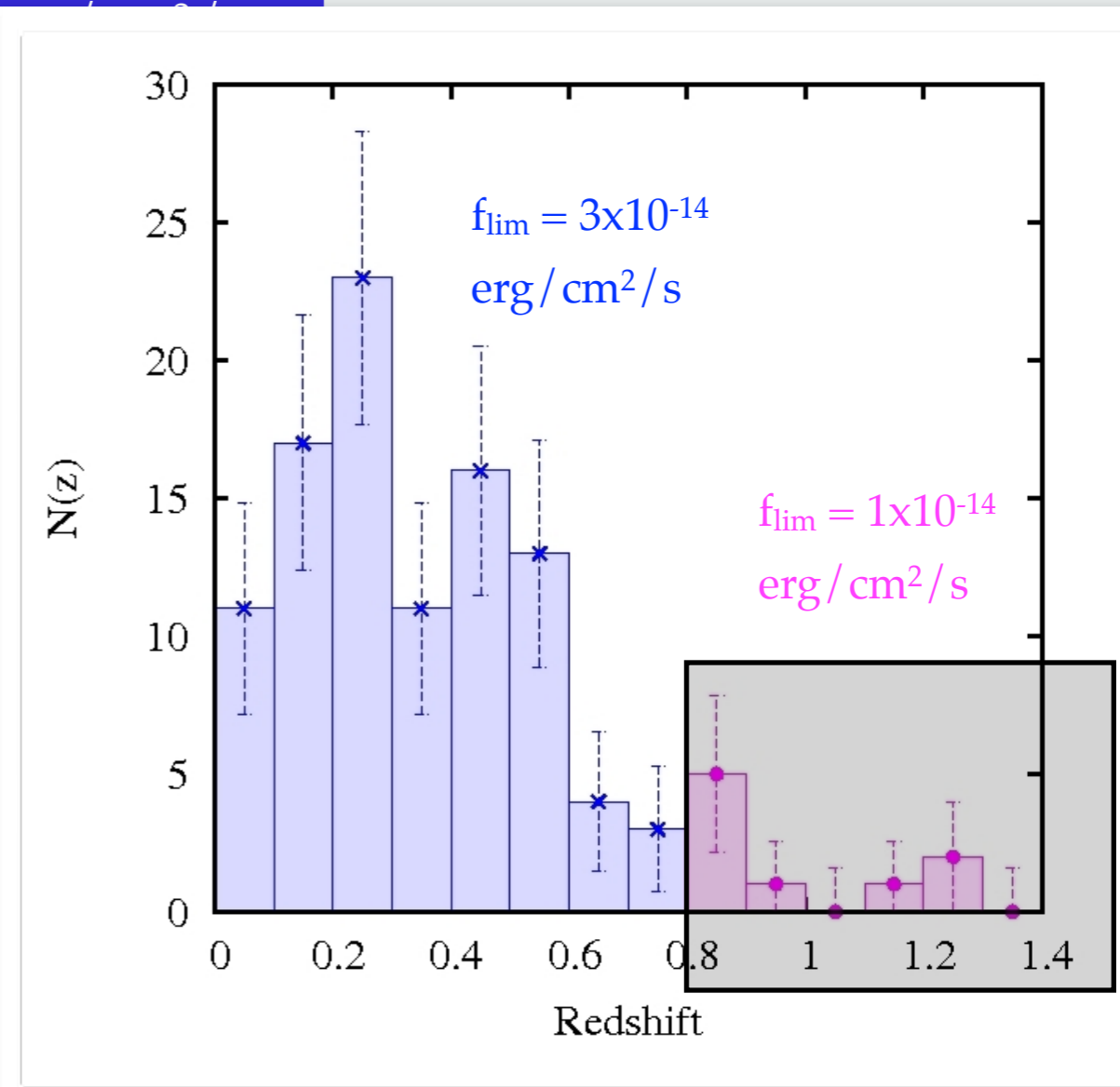
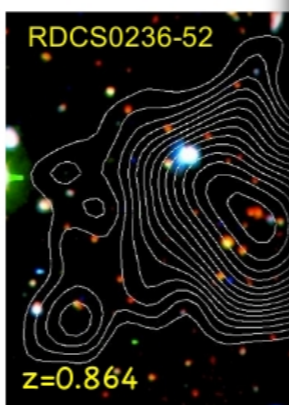
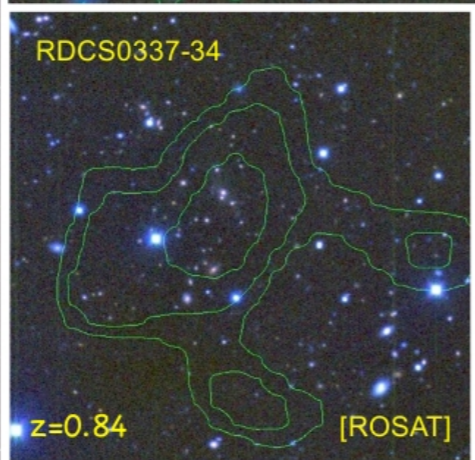
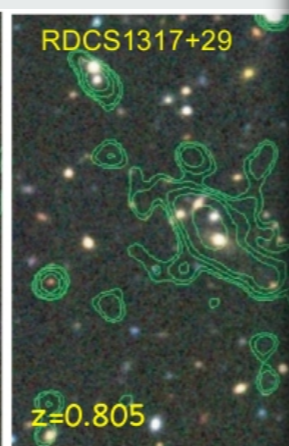
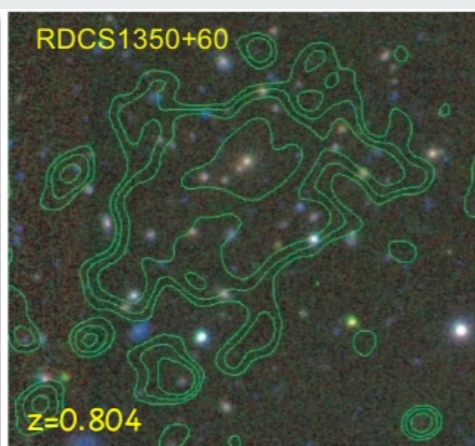
Rosati et al 1995

ROSAT Deep Cluster Sample - RDCS

RDCS redshift distribution ($N_{cl}=106$)

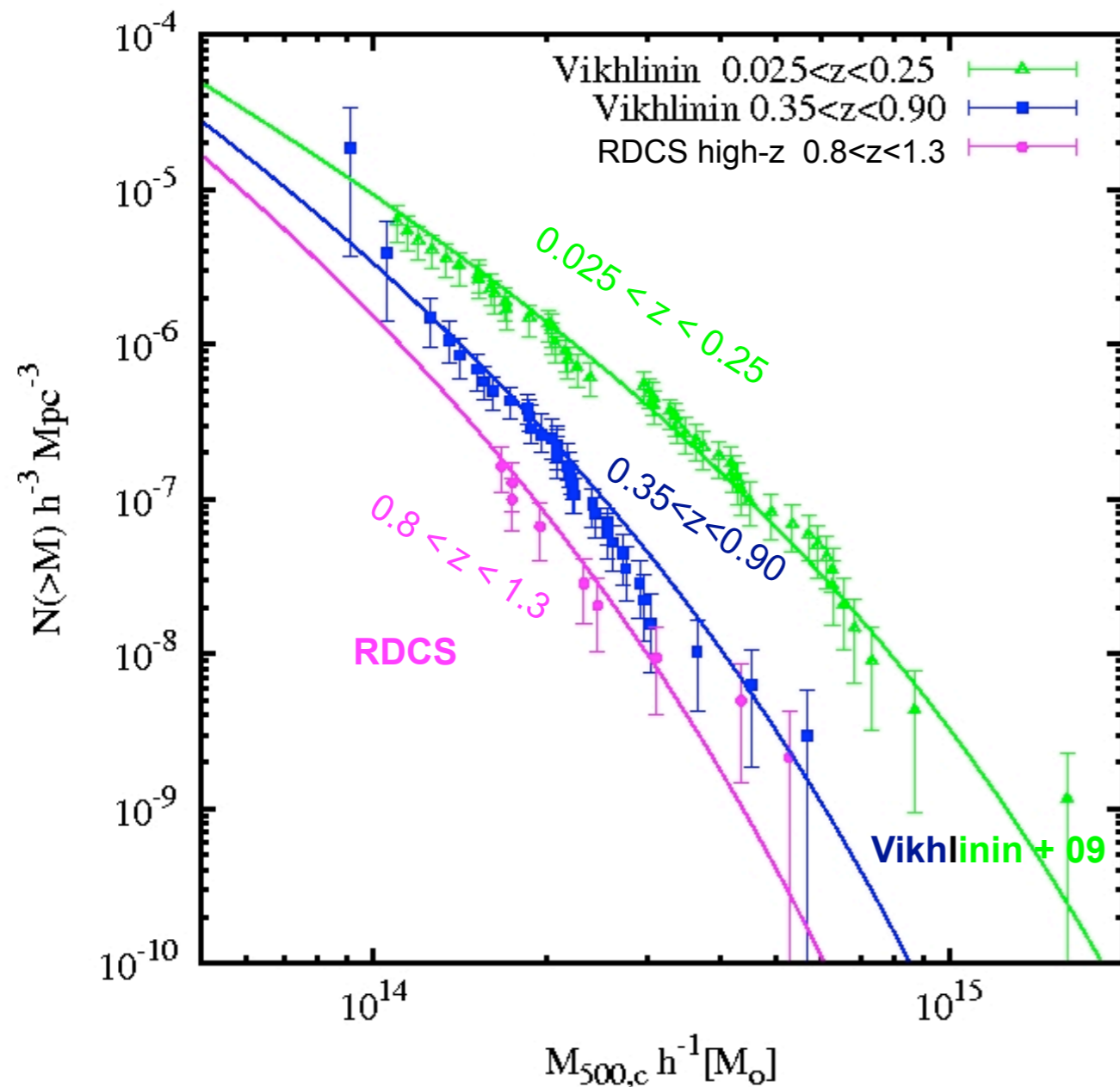


RDCS high-z sample
 $(f_{lim} = 10^{-14} \text{ erg/cm}^2/\text{s})$
 $[0.5 - 2] \text{ keV}$
 $0.8 < z < 1.4$



Rosati et al 1995

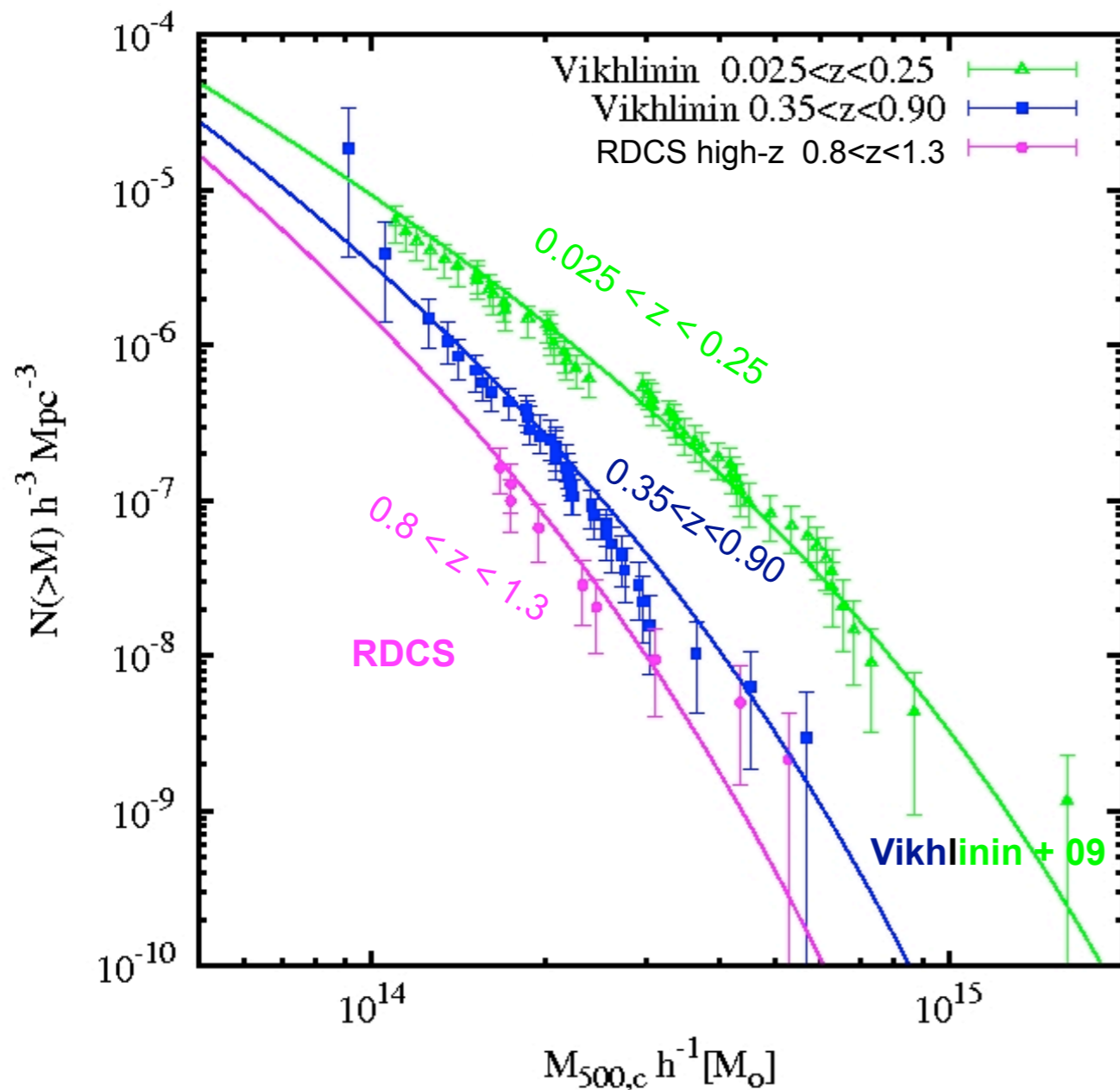
Cluster mass functions in three redshift ranges



- Mass from WL for 5 clusters from HST observations. Error on mass between $12\% < M_{\text{WL}} < 30\%$
- Mass from hydrostatic equilibrium for 7 clusters from Chandra observations. Error on mass between $20\% < M_{\text{X}} < 50\%$
- Mass derived from the theoretical observable-mass relations for 2 clusters. Error on mass $> 50\%$

Sartoris et al. 2012 in preparation

Cluster mass functions in three redshift ranges



$$N(>M) = \sum_{M_i > M} V(M_i)^{-1}$$

Rosat Deep Cluster Survey

($f_{\text{lim}} = 10^{-14}$ erg/cm²/s [0.5 – 2]keV band)

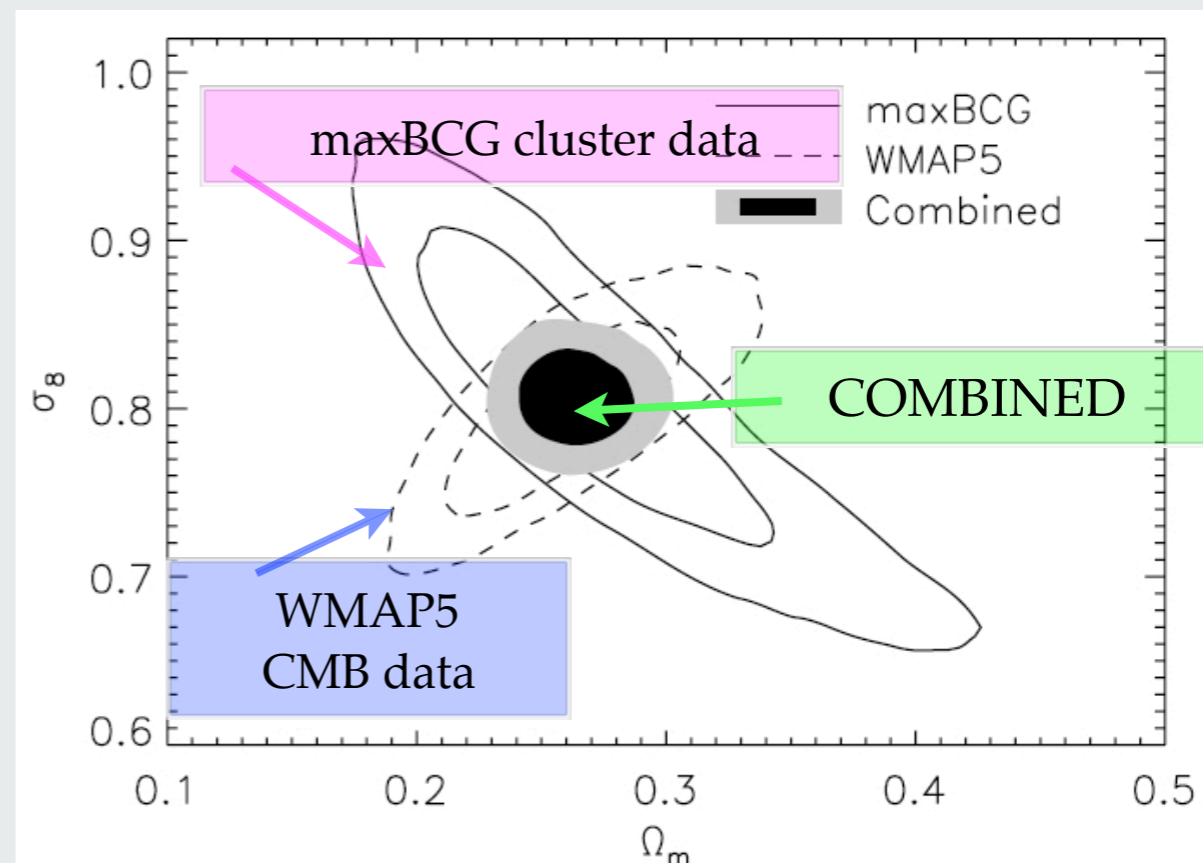
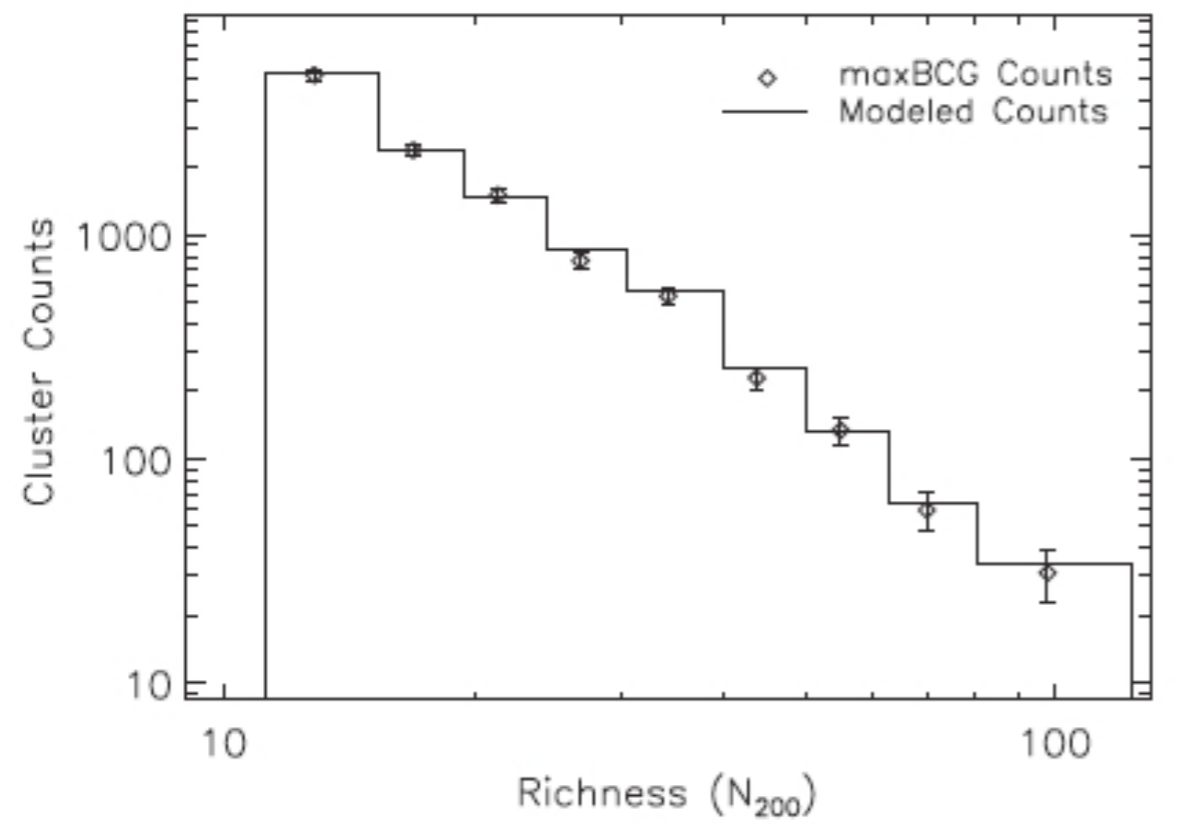
Cluster mass function at $\langle z = 0.9 \rangle$. The observed evolution of the mass function as calculated from zRDCS-1 sample is in agreement with prediction of Λ CDM at high redshift.

Sartoris et al. 2012 in preparation

Constraints from current optical survey: SDSS maxBCG

Rozo et al. (2010) derived cosmological constraints from the SDSS maxBCG cluster sample (Koester et al., 2007b) and the statistical weak lensing mass measurement from Johnston et al. (2007).

- SDSS maxBCG survey area: 7398 sq. deg.
- Photometric redshift range: [0.1, 0.3]
- More than 9×10^3 clusters



Conclusions

Forecast on DE EoS from future X-ray surveys:

- A robust measurement of the mass proxies and a large statistic of clusters are both important to obtain tight constraints.

Constraints deviation from Gaussian perturbation models with future X-ray surveys:

- NC and PS of galaxy clusters are highly complementary in providing constraints.
- PS is sensitive to deviations from Gaussianity, through the scale dependence of the bias.
- Wider area surveys better sample long-wavelength modes.

Tests of LCDM models with high redshift, massive cluster:

- Mass estimations from different methods are consistent and reduce possible systematic errors

Current X-ray cluster data:

- High- z mass function from current X-ray data confirm the LCDM scenario inferred from cluster samples at lower z . Waiting for cosmological constraints ...